

MASTER

Modelling and control of continuously adjustable shock absorbers for the imitation of passive dampers

van Gend, K.P.

Award date:
1997

[Link to publication](#)

Disclaimer

This document contains a student thesis (bachelor's or master's), as authored by a student at Eindhoven University of Technology. Student theses are made available in the TU/e repository upon obtaining the required degree. The grade received is not published on the document as presented in the repository. The required complexity or quality of research of student theses may vary by program, and the required minimum study period may vary in duration.

General rights

Copyright and moral rights for the publications made accessible in the public portal are retained by the authors and/or other copyright owners and it is a condition of accessing publications that users recognise and abide by the legal requirements associated with these rights.

- Users may download and print one copy of any publication from the public portal for the purpose of private study or research.
- You may not further distribute the material or use it for any profit-making activity or commercial gain

December 1, 1997

Modelling and control of continuously
adjustable shock absorbers
for the imitation of passive dampers

K.P.v.Gend

Graduation thesis
WFW report 97.076

Professor : prof. dr. ir. J.J. Kok
Coaches : dr. ir. F.E. Veldpaus
dr. ir. R.G.M. Huisman



Eindhoven University of Technology (TUE)
Department of Mechanical Engineering,
Division Systems and Control Engineering

Motto:

“I used to think that the brain was the most wonderful organ in my body. Then I realised who was telling me this.”

– Emo Phillips

Puzzle:

Computers are never stupid, sometimes the user just requests the impossible. I thought of an illustrative example in MATLAB:

```
>> [-5 : 0]
ans =
    -5    -4    -3    -2    -1     0
```

This is a common way in MATLAB to obtain a series of six values with increment unity. Let's extend this knowledge to another series:

```
>> [inf - 5 : inf]
```

The answer might prove different than you think. Most humans will apply the previous rule and write:

```
ans1 =
    Inf-5    Inf-4    Inf-3    Inf-2    Inf-1    Inf
```

But this is obviously wrong as infinity minus five equals to infinity. Some smarter people will still expect six values of infinity:

```
ans2 =
    Inf    Inf    Inf    Inf    Inf    Inf
```

Experienced programmers think more straight, first evaluating `inf-5` to `Inf` and consider the series `Inf : Inf` to contain only one value:

```
ans3 =
    Inf
```

You might think for yourself and guess the real answer. MATLAB can provide it, you might be astonished. Always remember the most important computer rule: “Garbage In = Garbage Out”.

Summary

During the design of new trucks, dampers need to be chosen for the truck suspension. Finding a correct damper consumes a lot of time as new dampers have to be inserted in a prototype over and over again, until sufficient performance is reached.

This report will deal with the development of a controller for a fast continuously adjustable shock absorber. By inserting this controllable damper in the prototype truck, one can specify the desired passive damper characteristics using a computer. This enables the test driver to test many passive dampers in short time.

First, various methods of damper parameter identification are described. It is concluded that all major methods are severely troubled by non-linear damper behaviour and temperature dependence and discard a lot of information.

In order to be able to use simulations in controller design, two damper models are derived. One using a white-box approach for a passive monotube damper. This model incorporates some non-linearities and temperature dependence.

The second model is developed using a black-box approach. The parameters of the controllable damper are fit using step responses. It is concluded that the parameters vary within large ranges, depending on the damper state.

To evaluate the performance of the controller/damper combination, several norms are discussed which directly compare the realised and desired damper forces. These do not match exactly. As the main goal states that a test driver is not allowed to notice the difference between a passive damper and the imitation of the passive damper by a controllable damper, a suspension and driver model are derived. Now driver accelerations can be compared, but due to the uncertainties on the sensitivity of test drivers, the resulting norms are rejected.

A PID-scheme is described as controller. Several enhancements are discussed. Simulations on three road profiles and several damper models show that output errors exist. There is too little information to decide whether the variable damper and its controller suffice.

Preface

This is my graduation report. I originally started September 1, 1996 with the project as a spin-off of the CASCOV project [19]. Fast continuously adjustable dampers were available for study and DAF was very interested in replacing the time consuming test driving with various passive dampers by test driving with the controlled dampers. Originally, modelling would be only a minor subject, the emphasis should lie on experiments using a real vehicle and some test rigs.

Unfortunately, the ÖHLINS dampers were fully booked for the CASCOV project. The CASCOV project also took more time than expected, it was completed in Fall 1997, instead of Winter 1997. I actually haven't even seen the ÖHLINS dampers. Therefore, the project became more theoretical, with a more profound modelling of the damper.

Begin May, 1997 I became ill. For three months, I was barely able to walk, let alone think about dampers and suspensions. The original deadline of August was set to December 1997. In the end of August, I was recovered enough to restart the research. This is the final result of it.

Many people have contributed to this report, partially by checking, proof reading and co-thinking, partially by moral support (and money). First of all, I would like to thank my parents and Sytske for all their faith in the outcome of my study and their 25+ years of work invested in me.

Both my coaches, Frans Veldpaus and Rudolf Huisman have spent many hours helping me to see through problems and correcting my intermediate reports. Without them, this report would never have existed. I would also like to thank Koenraad Reybrouck and Stefaan Duym at Monroe, Belgium for their explanations and the showing of real dampers and test facilities.

Gratitude also goes to Sven Pekelder, Bert van Beek, Vivian van Gansewinkel and Jeroen Heesakkers for proof reading of this thesis, help and lots of support.

Conny: Thanks for all the fish.

Finally, I would show gratitude to everybody who helped me and kept me going (again). Without all friends at the University, student's association Demos and the waterpolo team Nayade Heren Bier, it would have been very boring around here.

Contents

Summary	3
Preface	4
1 Introduction	7
1.1 Project goal	7
1.2 Outline of the thesis	7
1.3 Workings of a shock absorber	7
1.3.1 Passive damping	8
1.3.2 Active damping	9
2 Damper Characteristics and Parameter Identification	10
2.1 Introduction	10
2.2 Damper curves	10
2.2.1 The Pressure-Flow curve	10
2.2.2 The force-velocity curve	11
2.2.3 Work diagram	11
2.2.4 Restoring Force Surface	11
2.3 Identification methods	12
2.3.1 Harmonic excitation — VDA test	12
2.3.2 Stochastic excitation	14
2.3.3 Step responses	14
2.3.4 Constant Velocity-method	15
2.4 Hysteresis in shock absorbers	15
2.5 Conclusions	16
3 White Box modelling of passive dampers	17
3.1 Introduction	17
3.2 Modeling	17
3.2.1 Definitions	17
3.2.2 Oil	18
3.2.3 Gas	19
3.2.4 Piston	19
3.2.5 Heat	19
3.2.6 Flow	20
3.3 Model Assembly	21
3.4 Overview of Assumptions	22
3.5 Simulation Results	25
3.6 Conclusions	26
4 Black Box modelling of a controllable damper	28
4.1 Introduction	28
4.2 Interpolation	29
4.3 Gas spring	30
4.4 Oil Dynamics	30
4.5 Valve Dynamics	30

4.5.1	Introduction	30
4.5.2	First order valve dynamics	31
4.5.3	Second order valve dynamics	31
4.6	The second order damper model by Besinger	34
4.7	Performance of the first and second order damper models	35
4.8	Conclusions	35
5	Performance evaluation	37
5.1	Introduction	37
5.2	Suspension and driver model	37
5.3	Road profiles	38
5.4	Performance criteria	39
5.4.1	Performance from the driver's view	39
5.4.2	Performance from the damper's view	42
5.4.3	Discussion	44
5.5	Conclusions	46
6	Controller	47
6.1	Introduction and control objective	47
6.2	System definition	47
6.3	PID Controller	48
6.4	Results	49
6.5	Overshoot	50
6.6	Improvements	51
6.7	Other controller types	51
6.8	Conclusions	52
7	Conclusions and Recommendations	55
7.1	Conclusions	55
7.2	Recommendations	55
	Used References	57
A	Used Symbols	59
B	White Box Model: used parameters	61
C	Damper warming in the VDA-test	62
D	Results of fitting second order systems	63
E	Quarter Car model	64

1 Introduction

1.1 Project goal

During the design of a new prototype truck, the performance of the suspension can only be judged by building a prototype and inserting of a first guess shock absorber. Then a test driver evaluates the driving comfort and gives some advice on adjustments to the damper characteristics. Then the dampers are removed from the truck, adjusted and re-installed, after which the test driving starts again. The full process of replacing one set of dampers takes approximately two to three hours. During this time, the test driver is busy with nose-picking and forgetting the previous driving experience.

The general idea is to insert a fast continuously adjustable damper, which should be able to adjust itself to a desired damper force. Then it is possible to use this controllable damper as a replacement during test driving. Using a computer as controller, various passive damper characteristics can be evaluated in short time, thus enabling a shorter test drive phase in the design project.

As a spin-off of the CASCOV-project [9] [18] [19], fast controllable ÖHLINS dampers were available for study. But in contrast to the CASCOV project where the adjustable damper is used to obtain a higher level of comfort using information on the future road profile, this project only uses the controllable damper to mimic passive dampers.

The original project goal of developing a controller for damper imitation is not fully reached. The controller was only used in simulations and it remains unclear whether the controller suffices.

Although all discussions in this report concern the ÖHLINS damper, the systematics described in this report should be quickly portable to other dampers.

1.2 Outline of the thesis

The general workings of a shock absorbers are explained in Section 1.3 for both passive and adjustable dampers.

Several methods exist to characterise dampers. The differences are in input signals and the display of information: what is measured and what is discarded/neglected. This is discussed to a greater detail in Section 2.

In order to be able to use simulations for controller testing, a model of the ÖHLINS controllable damper has to be made. First, in Section 3, a so-called white model is derived for a passive damper only. Due to the absence of information of the workings of the controlled valve, the white box model could not be expanded to the controllable damper. Therefore, a black box model is used to obtain a model on the controllable damper in Section 4. Knowledge on the damper dynamics can also be used to select an appropriate controller type.

Section 5 discusses some methods to obtain performance criteria, i.e. norms to judge whether the test driver will notice the difference between a real passive damper and the ÖHLINS damper imitating the same passive damper. Finally, the implementation of a controller is discussed in Section 6. Simulation results are used to evaluate the performance.

1.3 Workings of a shock absorber

There are two kinds of shock absorbers: monotube dampers and twin-tube dampers. Twin-tube dampers are common in passenger cars because they are cheaper than monotube dampers.

In this report, only monotube dampers will be discussed as the damper involved — an ÖHLINS controllable damper — is of the monotube kind.

First, the passive monotube damper will be discussed. Afterwards, some extension will be made towards controllable dampers.

1.3.1 Passive damping

The essential mechanical parts of a passive monotube damper are a cylindrical tube and two pistons. (See Figure 1). Piston 10 separates compartment 2, filled with oil from compartment 3. Compartment 3 is filled with pressurised gas. This piston is called *floating piston*.

Piston 5 is connected to damper end 12 by rod 4. This piston can move in tube 13, which is connected to the other damper end 14. The pistons contains various small orifices and valves.

When a force is exerted on both damper ends, the damper will contract. Piston 5 moves, reducing the size of compartment 2 and enlarging the size of compartment 1. Oil must now flow from compartment 2 to 1, through the small orifices in the piston. An example of such orifice is 9.

Oil flow from compartment 1 to compartment 2 is called *rebound*, oil flow in the other direction is called *compression*.

There are also two larger one-way orifices in piston 5. One of those orifices opens if the pressure difference $\Delta p = p_1 - p_2$ exceeds a critical value, the so-called blow-off pressure.

The one-way orifices consist of a valve 9 and a spring. A stiffer spring will result in a higher blow-off pressure. The shape of valve 9 and the shape of inlet 7 are of major importance for the characteristics of the damper (See Section 2.2.2).

Oil flow through a small orifice results in a pressure loss. This means a loss of energy, which is converted into heat. This heat is transferred to the surroundings (air).

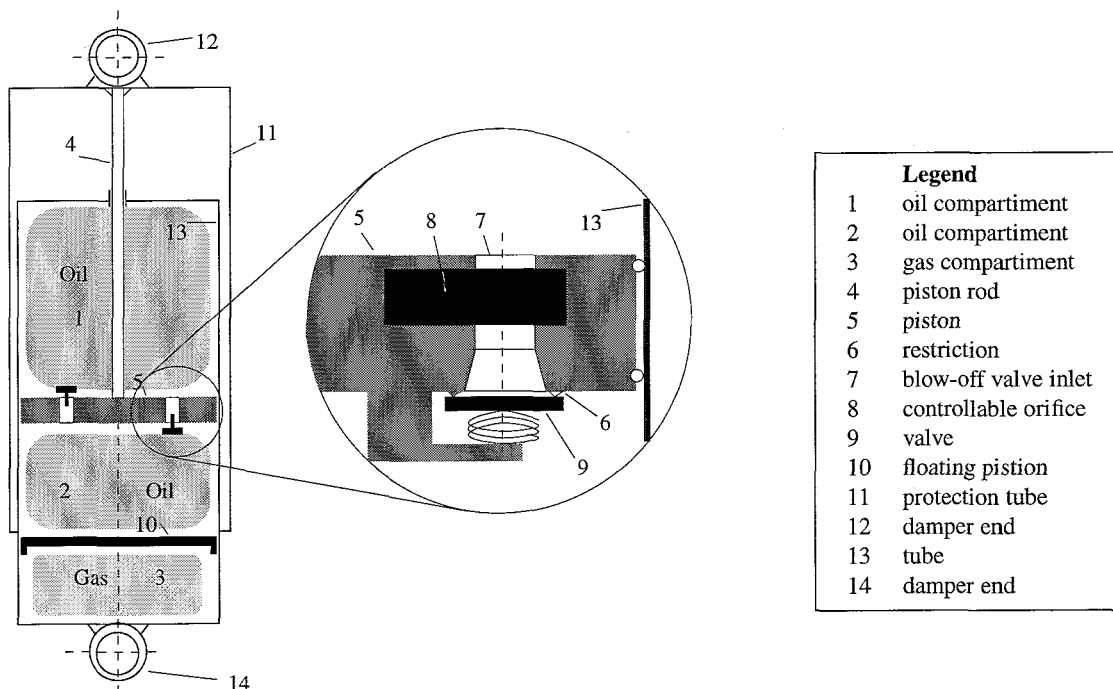


Figure 1: Schematic Drawing of a monotube damper.

1.3.2 Active damping

Recent developments have led to the development of controllable dampers. By using controllable dampers it is possible to change the behaviour of a shock absorber during the ride.

Early variable dampers, as used in the *Porsche 959* of the late eighties, contain two or three different fixed characteristics (See e.g. Reimpell und Stoll [20]), e.g. a luxury or sports-setting. During driving, these dampers can be set in accordance to the mood of the driver.

Later slow controllable dampers appeared. These can switch between characteristics fast enough to influence vehicle behaviour.

The ÖHLINS controllable damper is a *fast* controllable shock absorber. It is capable of fast switching: within a few milliseconds it can be adjusted continuously between a soft and a hard setting. This is accomplished by adapting the orifice area of the controllable orifice δ in Figure 1.

2 Damper Characteristics and Parameter Identification

2.1 Introduction

This chapter deals with some characteristics of monotube dampers and the methods to identify these characteristics. Section 2.2 will deal with the characteristics of a damper, specified in the form of the characteristic diagram (force-velocity curve), the work diagram (force-displacement curve) and the restoring force surface. Section 2.3 deals with common ways to obtain these curves. The subjects covered are harmonic excitation (VDA-test), stochastic excitation, step responses and constant velocity.

One of the non-linear effects of shock absorbers is called *Hysteresis*. In Section 2.4 is shown that various situations can lead to hysteresis.

2.2 Damper curves

2.2.1 The Pressure-Flow curve

When the piston of an automotive shock absorber is in motion, oil must flow through restrictions in the piston. This flow induces pressure differences between both sides of the piston. The resulting pressure difference causes the damper force.

The pressure-flow curve shows the influence of the restrictions and valves in the piston. The curve of a generalised damper is depicted in Figure 2). In this curve, three slopes can be distinguished. Each slope has its own behaviour:

- **Bleed:** oil can flow through small restrictions and leak past the piston. The pressure difference is proportional to the square root of the flow. (See Section 3.2.6 for details).
- **Blow-Off:** when the pressure difference between both oil compartments exceeds the blow-off pressure p_{br} at rebound, a blow-off valve will (partially) open. The shape of the valve and the stiffness of the spring influence the flow through the valve. This is discussed extensively by Reimpell und Stoll [20], Wößner and Causemann [29] and Lee [15] for some geometries. It is customary to design these valves such that the pressure-flow curve approximates a straight line during blow-off.
- **Restriction:** for pressure differences larger than some characteristic value p_{rr} (see Section 3.2.6), the blow-off valve is fully opened. Turbulent flow will result in a flow proportional to the square of

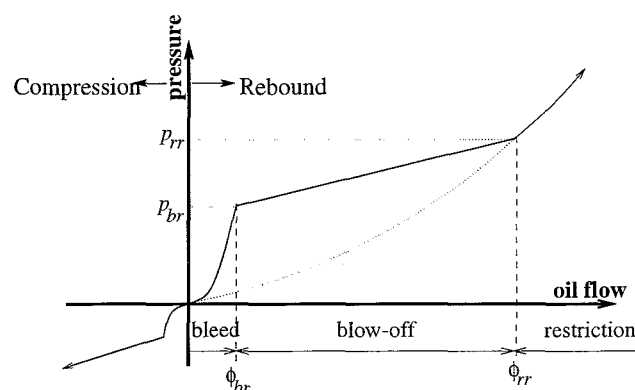


Figure 2: Damper characteristic curve

the pressure difference. This is similar to *bleed*, but with a different gain. Dampers for automotive use tend to have smaller rebound flows than compression flows, probably yielding better driving comfort.

2.2.2 The force-velocity curve

The main goal of a shock absorber is to dissipate energy. The dissipated energy within the time interval $[t_s, t_e]$ can be written as:

$$E = \int_{t_s}^{t_e} F_d(t) \dot{q}(t) dt \quad (1)$$

The damper force depends on the relative velocity \dot{q} and usually the damper behaviour can be described by means of a force-velocity curve. As the oil flow through the piston is closely related to the relative velocity and the damper force is closely related to the pressure difference, the resulting force velocity-curve looks very similar to the pressure-flow curve.

2.2.3 Work diagram

The work diagram is another way to represent damper behaviour. It is a force-displacement diagram, as can be seen in Figure 4. Usually, work diagrams are obtained using harmonic excitation of a shock absorber. This is discussed in the next section.

Among the effects to be distinguished in a force-displacement curve are “backlash” [24], which is due to friction and the valve dynamics, and damper hysteresis, caused by foaming of entrapped gasses in the damper oil or vapourization of the oil under low pressures. Damper hysteresis is discussed to greater detail in Section 2.4.

In Figure 4 it also can be seen that some kind of force-velocity curve can be derived from a set of work-diagrams, this is discussed in Section 2.3.1.

2.2.4 Restoring Force Surface

Assume a single degree-of-freedom non-linear system is governed by the equation of motion

$$m\ddot{y} + F(y, \dot{y}) = u(t). \quad (2)$$

If the time signals $y(t)$, $\dot{y}(t)$ and $\ddot{y}(t)$ and the excitation signal $u(t)$ are measured, one can determine the form of the non-linear restoring force F as a function of displacement and velocity. This function can be visualised as a surface in the displacement-velocity plane as depicted in Figure 3.

In practice, the requirement of the simultaneous measurement of acceleration, velocity and displacement appears to be a problem. It is easier to measure one of these quantities and estimate the other two. This is no trivial case. Worden [27] discusses various methods of integration and differentiation.

The demands on the excitation signal $x(t)$ are severe also. It should generate a phase trajectory $(y(t), \dot{y}(t))$ which covers as much of the phase plane as possible, to allow the construction of a continuous force surface. This is considered in detail by Worden in [28].

If the restoring force depends on other parameters than velocity and displacement only, the surface will look severely distorted. The surface is then replaced by a thin layer with thickness ϵ , describing the range of disturbances on the restoring force.

Recently Duym [4] proposed another RFS, representing the damper force as a function of velocity and acceleration, and advantageous especially for hysteresis fitting on broadband excitation signals.

2.3 Identification methods

To obtain the previously mentioned curves, experiments have to be conducted. A wide variety on possible tests is developed. A well-defined but ageing standard is the test standardised by the VDA which is discussed first.

Some of the tests described in this chapter, appear to be developed originally for linear systems. Other methods of characterisation do not use a-priori knowledge, introducing too many measurements (thus damper heating) which influence damper behaviour.

Using the knowledge gained in Section 3, far more sophisticated testing methods could be utilised.

2.3.1 Harmonic excitation — VDA test

Reimpell and Stoll [20], Huisman [9, chapter 3.1] and Hagendorn and Wallaschek [8] describe a standard procedure for determining the force-velocity-characteristic of a damper. This procedure is normalised by the VDA (*Verband der Automobilindustrie*) in Germany¹.

According to this “standard procedure”, a sinusoidal excitation is applied to the damper at various (standardised) frequencies. This can be accomplished by a relatively simple device (see Figure 5) consisting of a motor with an excenter hub. The standardised hub lengths are 25, 50, 75 and 100 [mm], whereas the number of revolutions is given by 25, 50, 75, 100, 150 and 200 [rpm]. The test sequence for the 100 [mm] hub excenter length is to revolve the hub six times at each speed and to measure only during each last revolution. Then the speed is increased, and the next six revolutions are made. The first five revolutions serve to make sure that the speed is correct and the air is released from the damper (especially important for twin-tube dampers, due to their open air contact). In Appendix C the heating

¹Unfortunately, the corresponding norms cannot be found.

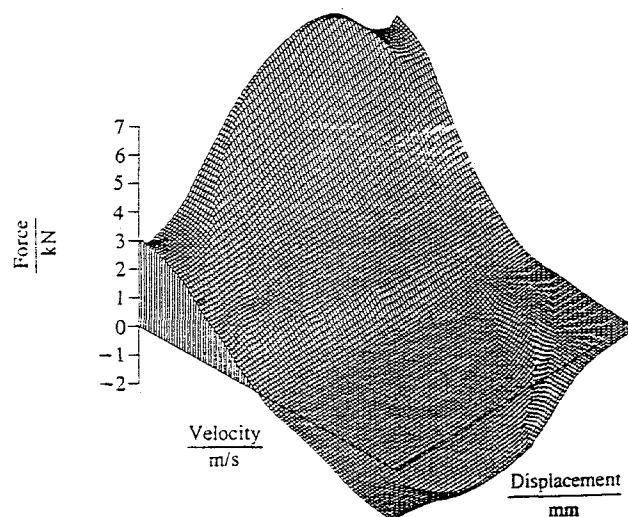


Figure 3: Restoring Force Surface. Plot taken from [24].

of the damper due to this excitation is calculated for a simplified damper model. As the sequence is standardised, influences from internal heating etc., are the same for all measurements.

In monotube dampers internal heating also influences the gas temperature. The gas compartment in a monotube damper is always pressurised, resulting in a static force on the damper. For the ÖHLINS damper, Huisman [9] observed static force variations between 50 and 500 [N], see also Section 3.5.

To generate the force-velocity curve, the maximum and minimal damper forces of the work diagram are used in combination with the relative velocities at that time to determine points on this curve (see Figure 4).

The VDA-test seems to be designed with (almost) linear dampers in mind. The test discards all information gained on damper hysteresis or instabilities due to velocity sign changes, etc. The test suits fine for a first impression of a damper, but is not useful for parameter estimation.

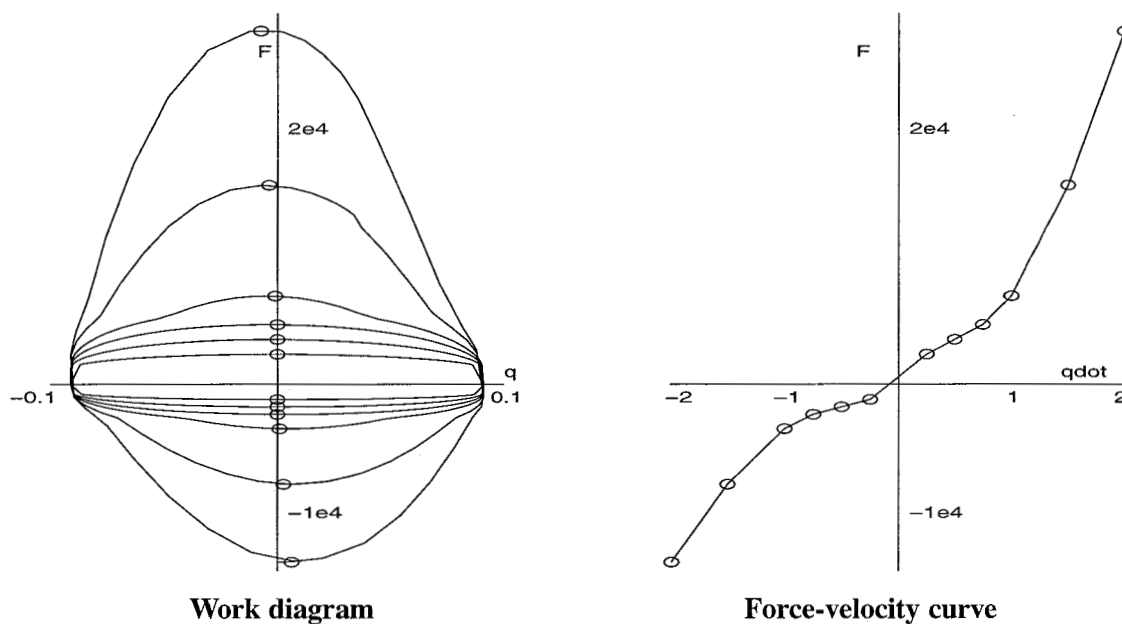


Figure 4: Standard procedure to determine a force-velocity curve by using a harmonic excitation.

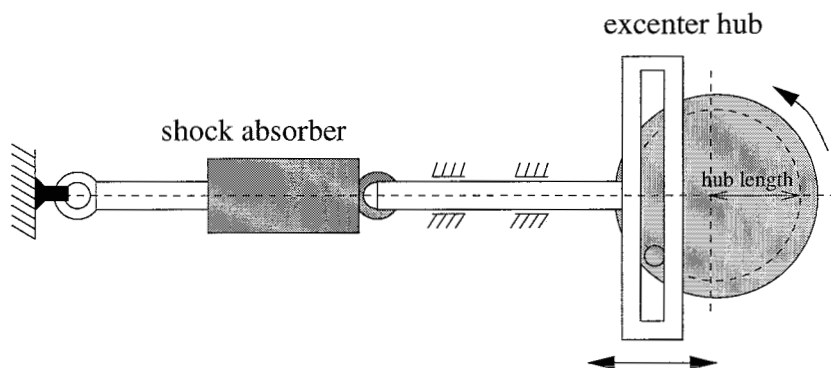


Figure 5: Schematic Drawing of VDA test equipment (rotated 90 degrees counterclockwise).

Worden [28] discusses the possible use of harmonic excitation to generate RFS-curves. Surace, Worden and Tomlinson [24] use harmonic excitation in combination with the RFS-technique for identification purposes on a parametric model which incorporates effects due to compressibility of oil in the damper.

Hagendorn and Wallaschek [8], [26] use harmonic linearization to derive linearized equations for use in multi-body full car models. Parameters are estimated using both harmonic linearization and stochastic linearization. They conclude that stochastic linearization provides more realistic results.

2.3.2 Stochastic excitation

Stochastic excitation can be used in two ways to accomplish parameter identification. The first method is to apply a stochastic input signal to a system and measure the responses. By comparing the input and the output in the frequency-domain, *linear* systems can be identified. For non-linear systems, however, this method is not suitable as there is no accurate method to describe most non-linear systems in the Laplace domain.

Cafferty, Worden and Tomlinson [3] use random excitation in combination with the RFS-method of system identification. They generate a stochastic signal as input signal to cover as much of the phase plane as possible within small time limits. The merits and demerits are:

- + Internal heating of the damper introduces non-stationary behaviour, as "it is known that absorbers are strongly temperature dependent". Using harmonic excitation, internal heating introduces non-linearities in the next sub test (at a different velocity). Stochastic excitation covers the phase plane much faster, with less damper heating, thus less induction of non-stationary behaviour (see also [28]).
- + It is unclear how isofrequency surfaces can be used to predict the response of the shock absorber under random excitation. Cafferty *et.al.* argue that using stochastic excitation results in better approximations of real damper behaviour, probably because the restoring force depends on more than displacement and velocity only. Stochastic excitation then excites this third influence in a more common way than harmonic excitation.
- The resulting surface is severely distorted. Five possible causes are discussed (amongst others cavitation and foaming of damping oil, inertia and unmeasured thermodynamic states). The latter cause is held responsible for distortion.

Stefaan Duym (employed by MONROE) mentioned in a personal interview that the influence of temperature during the stochastic excitation for an RFS was significant smaller than the influences introduced by manufacturing inaccuracies.

2.3.3 Step responses

The previous sections dealt with parameter identification on harmonic and stochastic signals. A third method is to use step responses.

According to Verbeek [25], shock absorbers in aircraft landing systems are tested using a drop test. A landing gear with an equivalent aircraft mass is released from a certain altitude to simulate impact with a prescribed vertical speed. The response of a system on a step on displacement (impulse in velocity) contains all eigenfrequencies of the system involved. This can be used to estimate the system's transfer function. Unfortunately, parameter estimation is severely troubled in the nonlinear case.

The origin of this kind of testing obviously lies in the design goal of aircraft landing gear: absorbing the energy of a landing aircraft. According to the PhD-thesis of Verbeek [25], using a shaker (i.e. harmonic excitation) is a more straightforward method for identification purposes.

2.3.4 Constant Velocity-method

It is also possible to measure the damper force for a constant velocity, induced for instance by hydraulic test equipment. Huisman [9] utilised this method. He noticed a strong influence of temperature and piston position on the measurements.

By using fast thermo-couples and a sophisticated test programme, it should be possible to measure the damper force using this technique, for a set of given temperatures. This would provide interesting information on the temperature-dependence of the damper.

2.4 Hysteresis in shock absorbers

In *AP Dictionary of Science and Technology* [17], hysteresis is defined as follows:

“A dependence of the state of system on its previous history, generally the retardation or lagging of an effect behind the cause of the effect.”

In common engineering practice, the phenomenon **hysteresis** is defined as the loss of energy when performing a closed loop around a point in e.g. a force-displacement diagram.

For example: to pull an ideal spring consumes energy. When the spring is released, **all** energy is returned. In case of hysteresis, some energy is lost. This can be seen in a force-displacement diagram as an enclosed area, see Figure 6. In an enclosed area, the loss of energy is described by (force \times displacement = work). Well known examples are dry friction (see Figure 7) or a damper parallel to a spring (see Figure 6).

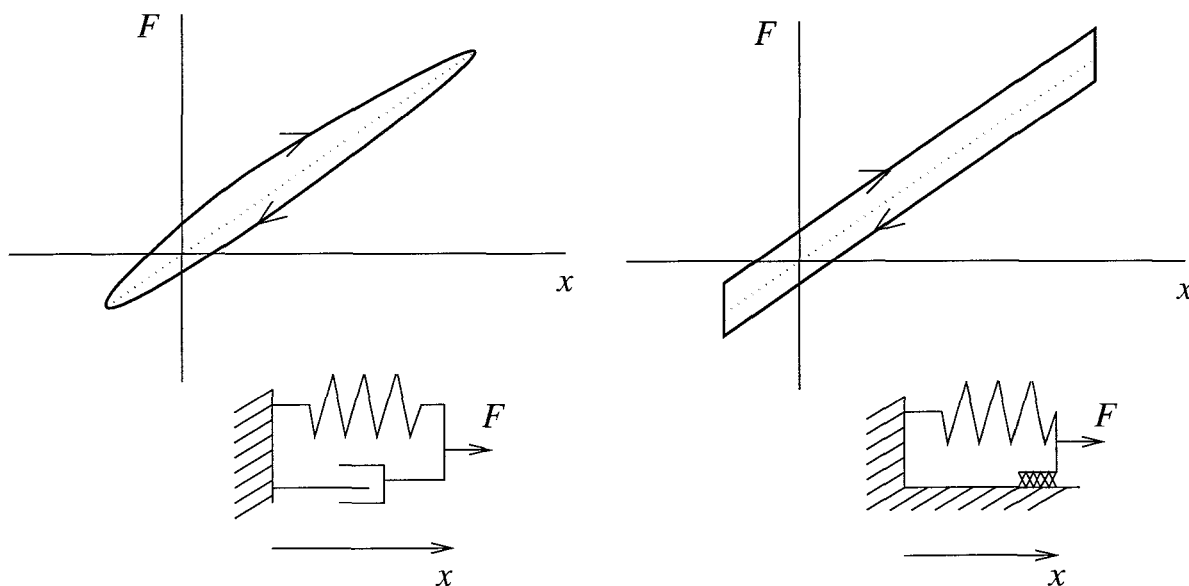


Figure 6: True hysteresis on a spring with a damper for a sawtooth force input signal.

Figure 7: True hysteresis on a spring with dry friction for a sawtooth force input signal.

In shock absorber engineering, it seems common to redefine hysteresis, see, e.g., Lang [14], Surace *et al.* [24]. They define an enclosed area in a force-velocity curve as hysteresis.

In this case, the exact inverse occurs: an ideal damper does not contain hysteresis, but a spring does. This is depicted in Figure 8. In this case a spring induces hysteresis and an ideal damper is hysteresis-free.

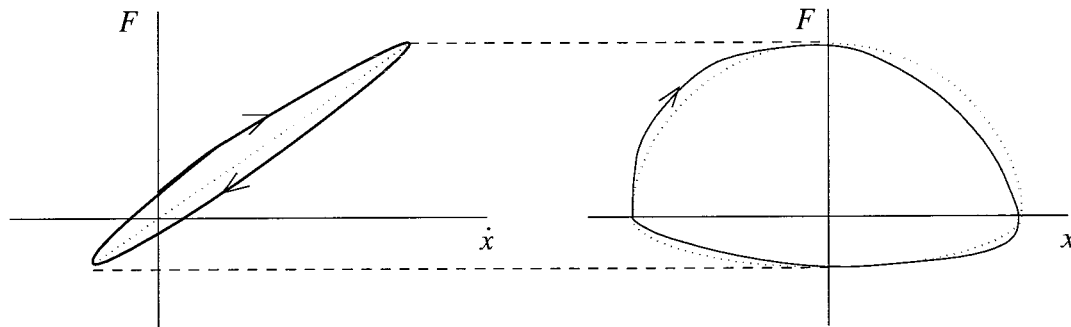


Figure 8: *Hysteresis according to the damper definition. Input signal is a sinusoidal displacement signal. To the left a force-velocity curve with hysteresis, to the right the corresponding force-displacement curve. The dotted line indicates the ideal curve.*

2.5 Conclusions

Currently three kinds of graphs are in use to show damper behaviour: force-velocity, force-displacement and force-velocity-displacement (3D-figure).

To obtain these curves, several types of experiments for parameter identification can be used. In most cases, the advantages or disadvantages break down to one simple conclusion: parameter identification is severely troubled by damper warming and non-linearities.

Most characterisation methods discard much of the gained information in order to create one of the graphs mentioned above.

3 White Box modelling of passive dampers

3.1 Introduction

The previous section discussed some methods to obtain damper curves, which showed non-linear effects and disturbances by e.g. temperature. In order to develop a controller, knowledge on the damper and the influence of the disturbances on its behaviour is very useful. Therefore, a damper model will be derived, starting from first principles in physics. A set of (differential) equations is derived, which together should describe the behaviour of a damper accurately enough. This is called “White Modelling”, as opposed to “Black Box”-modelling, a technique which only describes input-output behaviour of a system, thus NOT its contents. Black box modelling is used in Section 4 to model the controllable parts of a shock absorber.

The model equations are derived in Section 3.2. Emphasis is given to model some temperature dependencies, as the previous section made clear that temperature can strongly influence damper behaviour. An overview of all assumptions, together with a discussion on assumptions and results found in literature, is given in Section 3.4. Implementation of this model in a simulation environment and some simulation results can be found in Section 3.5. This section also covers the resulting temperature dependence and the static force of the damper model.

3.2 Modeling

3.2.1 Definitions

A monotube damper consists of a closed tube, assumed to be rigid with constant volume V_d . In this damper there are two pistons for the separation of three compartments. Piston 1 is connected to the piston rod and has a constant volume V_{p1} . Piston 2 with volume V_{p2} is a floating piston, separating the oil compartment 2 from the gas compartment 3. The area of the pistons is constant and denoted by A_p , the cross sectional area of the connecting rod is A_r .

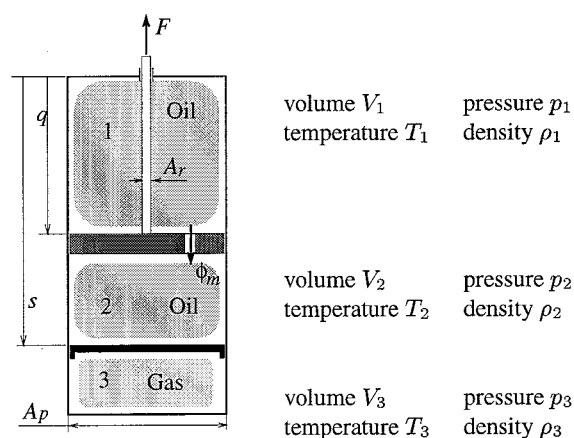


Figure 9: Definition of shock absorber characteristics.

The volume of compartments 1 to 3 is given by:

$$V_1 = \{A_p - A_r\} q; \quad (3)$$

$$V_2 = A_p \{s - q\} - V_{p1}; \quad (4)$$

$$V_3 = V_d - V_{p2} - A_p s; \quad (5)$$

Sign definitions for the position coordinates q and s of piston 1 and piston 2 are given in Figure 9.

3.2.2 Oil

The mass balances of compartments 1 and 2 yield:

$$\frac{d}{dt}(\rho_1 V_1) = -\phi_{m12} \quad (6)$$

$$\frac{d}{dt}(\rho_2 V_2) = +\phi_{m12} \quad (7)$$

where ϕ_{m12} is the mass flow from compartment 1 to compartment 2 and ρ_i is the oil density in compartment i ($i = 1, 2$).

The density is a function of the pressure p and the temperature T , i.e.

$$\rho = h(p, T) \quad (8)$$

Hence, the rate $\dot{\rho}$ of ρ is related to the rates \dot{p} and \dot{T} by

$$\frac{\dot{\rho}}{\rho} = -\alpha_{oil} \dot{T} + \beta'_{oil} \dot{p} \quad (9)$$

where the coefficients α_{oil} and β'_{oil} follow from:

$$\alpha_{oil} = -\frac{1}{h} \left(\frac{\partial h}{\partial T} \right)_p \quad (10)$$

$$\beta'_{oil} = \frac{1}{h} \left(\frac{\partial h}{\partial p} \right)_T \quad (11)$$

The **compressibility factor** β'_{oil} (see Janna [12, equation 7.6]) is set to zero, which means that the oil density is independent of pressure. The **volumetric thermal-expansion coefficient** α_{oil} is assumed to be independent of pressure and temperature. Hence, the density is given by:

$$\rho(T) = \rho(T_0) e^{-\alpha_{oil}\{T-T_0\}} \quad (12)$$

Substitution in equations (6) and (7), results in:

$$-\phi_{m12} = \rho_1 \{A_p - A_r\} \dot{q} - \alpha_{oil} \rho_1 \{A_p - A_r\} q \dot{T}_1 \quad (13)$$

$$+\phi_{m12} = \rho_2 A_p \{\dot{s} - \dot{q}\} - \alpha_{oil} \rho_2 [A_p \{s - q\} - V_{p1}] \dot{T}_2 \quad (14)$$

3.2.3 Gas

The gas in compartment 3 is assumed ideal, with specific gas constant R and specific heat at constant volume c_v . The ideal gas law states:

$$p_3 V_3 = m_g R T_3 \quad (15)$$

Various models in literature (see e.g. Reybrouck [21] and Lee [15]) assume adiabatic conditions, i.e. no heat is exchanged between the gas and the damper. One of the primary targets of this model is to incorporate temperature effects: so this assumption is rejected here.

The energy balance law for the gas volume is:

$$\begin{aligned} \left(\begin{array}{c} \text{Accumulation} \\ \text{of Heat} \end{array} \right) &= \left(\begin{array}{c} \text{Net rate of work} \\ \text{done by system} \\ \text{on surroundings} \end{array} \right) + \left(\begin{array}{c} \text{Flow of heat} \\ \text{towards system} \end{array} \right) \\ \rightarrow m_g c_v \dot{T}_3 &= -p_3 \dot{V}_3 - Q_g \end{aligned} \quad (16)$$

where m_g is the mass of the gas in compartment 3 and Q_g is the flow of heat.

The combination of equations (15) and (16) results in:

$$m_g c_v \dot{T}_3 = -m_g R \frac{\dot{V}_3}{V_3} T_3 - Q_g \quad (17)$$

where V_3 is defined earlier in (5).

3.2.4 Piston

To model the force equilibrium on both pistons, two simplifying but realistic assumptions are made:

- The mass of both pistons is negligible.
- Friction between the pistons and the tube is negligible.

Then the equations of motion for the pistons become:

$$F = \{A_p - A_r\} p_1 - A_p p_2 \quad (18)$$

$$0 = A_p p_2 - A_p p_3 \quad (19)$$

This implies that p_2 will always equal p_3 .

3.2.5 Heat

In the previous sections, three temperatures T_1 , T_2 , T_3 are used. It is assumed that, because of the piston movement, the oil in compartment 1 and 2 is well mixed. As the thermal conductivity of metals is much higher than that of oil or gas, the whole tube is assumed to be at one temperature, which equals the temperature of the oil, so

$$T_1(t) = T_2(t) = T_{tube}(t) \quad (20)$$

Since the oil density ρ_i in compartment i ($i = 1, 2$) is assumed to depend on the oil temperature T_i in compartment i only, this implies that $\rho_1(t) = \rho_2(t)$.

In general, the variation of $T_{tube}(t)$ is much slower than the variations of $q(t)$ and $s(t)$. Therefore it is assumed that the influence of $\dot{T}_{tube}(t)$ is negligible. More precisely, it is assumed that the term $\dot{\rho}_i V_i$

in equations (6) and (7) is small compared to the term $\rho_i \dot{V}_i$. Then it is readily seen that $\dot{V}_1(t) = \dot{V}_2(t)$. Using equation (5) it follows that:

$$A_p \dot{s}(t) = A_r \dot{q}(t) \quad \dot{V}_3(t) = -A_r \dot{q}(t) \quad (21)$$

$$s(t) = s_0 + \frac{A_r}{A_p} q(t) \quad V_3(t) = A_r \{q_{max} - q(t)\} \quad (22)$$

where s_0 is the position of the floating piston for $q = 0[m]$, and $A_r q_{max}$ is the maximum volume of the piston rod within the damper tube, or the gas volume at $q = 0$. Note that for $q = q_{max}$, the gas volume should be reduced to zero, thus being only a fictitious position.

Note that T_{tube} still can vary with respect to time! (So-called quasi-stationary).

The rate of change of the temperature T_3 of the gas may not be neglected. A temperature difference between T_3 and T_{tube} will result in a heat flow Q_g . This is modelled using Newton's Law of Cooling (see Janna [12, Section 1.6]):

$$Q_g(t) = \bar{h}_c A(t) \{T_3(t) - T_{tube}(t)\} \quad (23)$$

where \bar{h}_c , the **average convection heat transfer coefficient**, accounts for the overall effects embodied in the process of convection heat transfer. Furthermore, the area $A(t)$ is the area of heat transfer between gas and tube, i.e.

$$A(t) = 2 A_p + 2 \sqrt{\frac{\pi}{A_p}} V_3(t) \quad (24)$$

In normal operation, differences in $A(t)$ are relatively small, so equation (23) can be simplified to:

$$Q_g(t) = \lambda_g \{T_3(t) - T_{tube}(t)\} \quad (25)$$

3.2.6 Flow

The oil flow ϕ_v in **rebound**², i.e. for $\dot{q} < 0$, from compartment 1 to compartment 2 depends on the pressure difference $p_1 - p_2$. Depending on the magnitude of this difference, there are three possible situations.

Bleed on rebound

For $p_1 - p_2 < p_{br}$ (where p_{br} is the blow-off pressure at rebound), the blow-off valve is closed. In this case, oil can flow through restrictions (like δ in Figure 1) and leak past the piston. This is called **bleed**. If turbulent flow through the restrictions is assumed (see also Section 3.4), this can be written as:

$$\phi_{v12} = \frac{\phi_{m12}}{\rho_{oil}(T_{tube})} = k_{rb}(T_{tube}) \{p_1 - p_2\}^n \quad (26)$$

where $n = \frac{1}{2}$ for standard steady turbulent flow (Lang [14]). The rebound bleed constant $k_{rb}(T_{tube})$ is defined as:

$$k_{rb}(T_{tube}) = C_d(T_{tube}) A_{res} \sqrt{\frac{2}{\rho_{oil}(T_{tube})}} \quad (27)$$

Here, A_{res} is the area of the restrictions and C_d accounts for geometry effects of the orifices (Reynolds-number, etc.).

²The same discussion can be held for **compression** ($\dot{q} > 0$).

Restriction on rebound

When the blow-off valve is fully opened, i.e. $p_1 - p_2 \geq p_{rr}$, the whole of restrictions, valves and leakage can be seen as one large orifice. The assumptions from **bleed** do also apply here, resulting in:

$$\phi_{v_{12}} = k_{rr}(T_{tube})\{p_1 - p_2\}^n \quad (28)$$

with $n = \frac{1}{2}$. The difference between (28) and (26) is in the parameters k_{rr} and k_{rb} , where $k_{rr} \gg k_{rb}$.

Blow-off on rebound

For $p_{br} \leq p_1 - p_2 < p_{rr}$, the blow-off valve is partially opened. The total flow through the piston will range between the maximum blow-off flow ϕ_{br} and the minimal restriction flow ϕ_{rr} , which by definition are given as follows:

$$\phi_{br}(T_{tube}) := k_{br}(T_{tube})\sqrt{p_{br}} \quad (29)$$

$$\phi_{rr}(T_{tube}) := k_{rr}(T_{tube})\sqrt{p_{rr}} \quad (30)$$

By adjusting the shape of the valve and orifice and the stiffness of the valve springs, the characteristics of the flow through the valve can be adjusted. This is discussed by Lang [14, Section 3.3] in great detail. Lee [15] models a deflecting disk-restriction.

In general, for automotive shock absorbers, the characteristics during blow-off are adjusted to provide a somewhat linear relationship within the range $(p_{br}, \phi_{br}) \dots (p_{rr}, \phi_{rr})$. It is assumed that such characteristic is fully linear:

$$\phi_{v_{12}} = \frac{\{p_1 - p_2\} - p_{br}}{p_{rr} - p_{br}} \{\phi_{rr} - \phi_{br}\} + \phi_{br} \quad (31)$$

3.3 Model Assembly

All relations necessary for the model have been derived in the previous sections. However, many of the parameters within the model are superfluous. In order to present a compact model, some equations have to be rewritten. All equations necessary for the model are:

- The assumption in (20) reduced (13) to:

$$\phi_{v_{12}} = -\{A_p - A_r\}\dot{q} \quad (32)$$

- Inserting equations (22) and (21) into (17) yields:

$$m_g c_v \dot{T}_3 = m_g R T_3 \frac{\dot{q}}{q_{max} - q} - \lambda_g \{T_3 - T_{tube}\} \quad (33)$$

- All three cases of oil flow through the piston (26), (28), (31) can be lumped into one equation. Insertion of (29) and (30) results in:

$$\phi_{v_{12}} = \begin{cases} \phi_{br} \sqrt{\frac{p_1 - p_2}{p_{br}}} & \text{for } 0 \leq p_1 - p_2 \leq p_{br} \\ \phi_{br} + \frac{p_1 - p_2 - p_{br}}{p_{rr} - p_{br}} \{\phi_{rr} - \phi_{br}\} & \text{for } p_{br} \leq p_1 - p_2 \leq p_{rr} \\ \phi_{rr} \sqrt{\frac{p_1 - p_2}{p_{rr}}} & \text{for } p_1 - p_2 \geq p_{rr} \end{cases}$$

However, for most applications, the inverse of this equation is needed as the oil flow is known from the relative velocity of the piston (equation (32)). The inverse is:

$$p_1 - p_2 = \begin{cases} p_{br} \left\{ \frac{\phi_{v12}}{\phi_{br}} \right\}^2 & \text{for } 0 \leq \phi_{v12} \leq \phi_{br} \\ p_{br} + \frac{\phi_{v12} \phi_{br}}{\phi_{rr} - \phi_{br}} \{p_{rr} - p_{br}\} & \text{for } \phi_{br} \leq \phi_{v12} \leq \phi_{rr} \\ p_{rr} \left\{ \frac{\phi_{v12}}{\phi_{rr}} \right\} & \text{for } \phi_{v12} \geq \phi_{rr} \end{cases} \quad (34)$$

Please note that ϕ_{rr} and ϕ_{br} still depend on the temperature T_{tube} (see (27) to (30)).

- Combination of (19), (15) and (22) results in a relation for p_2 :

$$p_2 = \frac{m_g R T_3}{A_r \{q_{max} - q\}} \quad (35)$$

- Equation (18), equation of motion for piston 1 remains unchanged:

$$F = \{A_p - A_r\} p_1 - A_p p_2 \quad (36)$$

Equations (32) to (36) represent the full model for **rebound**.

Please note that the model is not compared to the actual ÖHLINS damper. This was impossible because at the time the model was finished, the dampers had to be returned to the manufacturer. Thus the model is not validated.

3.4 Overview of Assumptions

In the previous sections, a number of assumptions has been made. In this section, these assumptions are compared to assumptions found in Lang [14], Wallaschek [26], Hagendorn and Wallaschek [8], Janna [12], Reimpell und Stoll [20], Mitschke und Riesenberg [16], Lee [15], Reybrouck [21] and Duym et al. [5].

The symbols used in the following table in front of the remarks have the following meanings:

- + The remark confirms the assumption of this report.
- The remark neither contradicts nor confirms the assumption.
- The remark contradicts the assumption.

In:	Assumption:	Verification:
§ 3.2.1	Tube volume constant, piston volume constant.	<input type="checkbox"/> <i>Lang</i> models expansion and contraction of the cylinder walls due to changes in pressure [14, Section 3.1].
§ 3.2.2	Oil is incompressible.	+ <i>Wallaschek</i> also assumes incompressibility. – <i>Surace et al.</i> use compressibility of the fluid to explain hysteresis. – <i>Lang</i> shows that the hysteresis loops in force-velocity diagrams, at higher frequencies, are caused by the compressibility of the shock absorber fluid and the expansion and contraction of a gas phase in the compression and rebound chamber. See [14, Section 6.9].
§ 3.2.2	The volumetric thermal-expansion coefficient α_{oil} is independent of oil temperature.	+ <i>Janna</i> gives only one α_{oil} for engine oil for temperatures ranging from 0 to 160 [°C] [12, Table C.4].
§ 3.2.2	Liquid oil is the only medium in compartments 1 and 2.	– According to <i>Wallaschek</i> , on a velocity sign change, an equalisation of pressures must occur before flow between the chambers can reverse. <i>Lang</i> observed the appearance of gas bubbles in the oil. Further investigation revealed that it was not vaporised oil, but dissolved gas (entrapped air) in the liquid. This phenomenon is modelled by <i>Duym</i> for twin-tube dampers. <input type="checkbox"/> In a monotube-damper no oil-air contact is possible. In proper damper manufacturing, oil should not contain entrapped air. Besides, generally, the high internal pressure of a monotube damper will prevent the appearance of the bubbles.
§ 3.2.3	The gas in compartment 3 is ideal.	+ The same assumption is made by <i>Reybrouck</i> , whose damper has a static gas pressure of $6.9 \times 10^5 [Pa]$.
§ 3.2.3	The gas in compartment 3 obeys the ideal gas law.	<input type="checkbox"/> Both <i>Reybrouck</i> and <i>Lee</i> use an adiabatic gas law, assuming there is no heat exchange between the tube and the nitrogen gas. This assumption greatly simplifies their equations. However, one of the goals of this model is to investigate temperature-influences.

(continued on next page)

(continued from previous page)

In:	Assumption:	Verification:
§ 3.2.4	The mass of the pistons is negligible.	<p>+ <i>Wallaschek</i> reasons that the piston is connected to the chassis of a vehicle, whilst the tube is connected to the axle. In both cases, the added inertia of the damper is negligible.</p> <p><input type="checkbox"/> The previous remark is not applicable to the floating piston, but $m_{p2} \ddot{s} \ll p_3 A_p$.</p>
§ 3.2.4	Friction is negligible.	<p>– All authors incorporate friction, mostly Coulomb friction.</p> <p>+ According to <i>Reybrouck</i>, friction is only important at low velocities.</p>
§ 3.2.2 § 3.2.5	The temperature of the oil and the metal parts of the damper are the same.	<p><input type="checkbox"/> Most authors neglect the influence of temperature. According to <i>Lang</i>, this is because it strongly increases model complexity.</p> <p>+ <i>Mitschke und Riesenberg</i> claim that the temperature difference between tube and oil is small for mono-tube dampers.</p>
§ 3.2.5	The time scale of changes in T_{tube} is much larger than the time scale of changes in q or s .	
§ 3.2.6	Oil flow through restrictions and valves is turbulent.	<p>– <i>Wallaschek</i> and <i>Surace et al.</i> assume laminar flow; throttle losses are dealt with in a separate equation.</p> <p>+ <i>Reybrouck</i> notes that turbulent flow is valid for excitation signals from 0.5 [Hz] up to 30 [Hz].</p> <p>+ <i>Mitschke und Riesenberg</i> claim that damper engineers try to avoid laminar flow because of its higher temperature dependence.</p>
§ 3.2.6	All orifices and leaks are lumped into one orifice.	<input type="checkbox"/> <i>Lang</i> arguments that leakage is almost negligible.

3.5 Simulation Results

The model derived in Section 3.3 is also implemented for simulations using SIMULINK. For that purpose, the damper model was rewritten in state-space representation. Some additional, simplifying assumptions were made:

- The influence of the temperature T_{tube} on the damper fluid through the valves (27) is neglected.
- The same model was used for both rebound and compression. However, for compression the pressure difference in (36) was reduced to only 1/3 of its real value, resulting in far lower damper forces in compression.

Parameters of the simulated model can be found in Appendix B.

Please note that no effort was made to compare the model or its parameters to the actual ÖHLINS damper. This was impossible because at the time the model was finished, the dampers had to be returned to the manufacturer. Thus the model is not validated.

Simulation of VDA test

For harmonic excitation as specified in the VDA-test (see Section 2.3.1), the force-velocity curve was simulated. The resulting curve is depicted in Figure 4. Note that the test was simulated at a constant tube temperature $T_{tube} = 293[K]$ ³. Due to damper hysteresis, the force-displacement curve is NOT symmetrical.

Influence of temperature

The nitrogen gas is warmed and cooled by its surroundings: the damper tube. To investigate the resulting gas behaviour, an harmonic excitation with a hub of 0.1 [m] rotation at 100[rpm] was performed for two different but constant tube temperatures: 273 [K] and 323 [K].

In Figure 10, the difference between the gas temperature and the tube temperature is printed. In both cases, the gas had an initial temperature of 293 [K]. It can be seen that the transient response of the gas temperature is damped out quite fast: within 0.2 [s].

The ratio of the amplitudes of both curves is exactly 323/273, i.e. the amplitude is proportional to the tube temperature. The resulting extra damper force due to this temperature raise is negligible.

Static force

The static damper force is the force exerted by the damper *in rest*, i.e. $F(\dot{q} = 0)$. Huisman and Vissers [9] wrote that:

“During the measurements the static force varied between 50 and 500 [N] depending on the damper temperature.”

However, using the model from Section 3.3, these results seem unlikely.

In rest (i.e. $\dot{q} = 0[m/s]$), no pressure difference $p_1 - p_2$ exists:

$$p_1 = p_2 = p_3 \quad (37)$$

Inserting (37) and (35) into (36) result in:

$$F = \frac{-m_g R}{q_{max} - q} T_3 \quad (38)$$

³Increase of the damper temperature (as a result from the energy dissipation) would have lead to gas pressure increase only, as the dependence of fluid properties on temperature was not included in the simulation.

So within the range of damper temperatures ($0..60[^\circ C]$), the damper force will vary about 20 %. Additional effects like the expansion of the oil will add 10% to this variation of the damper force.

However, the static force is highly position-dependent: for q within close range of q_{max} , the denominator of (38) goes to zero, inducing a strong increase in F (For $q = q_{max}$, no space is left for the gas, resulting in a infinite pressure).

The same effects can be seen in the simulations. Using the parameters from Appendix B, the parameter q_{max} was $0.4393[m]$. Results from the simulations are given in Figure 11.

3.6 Conclusions

In this section, a “white” damper model is derived. In contrast to damper models found in literature (most of which are valid for isothermal dampers only) the influence of temperature on damper behaviour is incorporated. Dampers are known to show different non-linear behaviour at different temperatures, which might be partially explained using this model.

The assumptions made are compared to assumptions made in literature. All assumptions seem to hold.

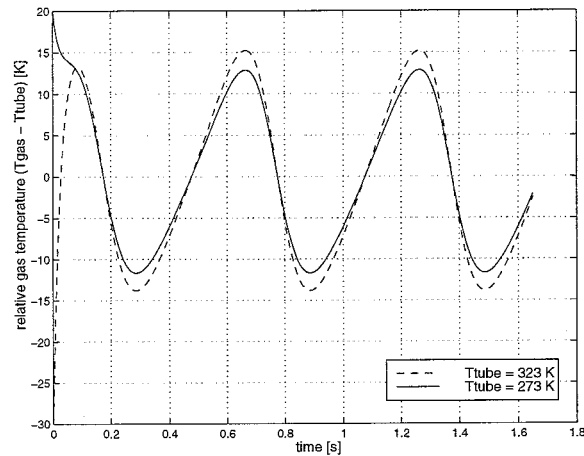


Figure 10: Relative gas temperatures ($0 \equiv 293[\text{K}]$) on a harmonic excitation for two different tube temperatures.

q [m]	T_{tube} [K]	F [N]
0.0	273	-47.7
0.0	293	-51.2
0.0	323	-56.5
0.2	273	-87.7
0.2	293	-94.0
0.2	323	-103.5
0.4	273	-543
0.4	293	-573
0.4	323	-631

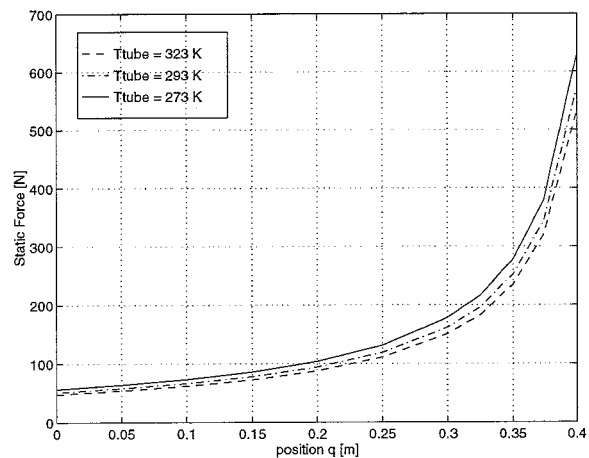


Figure 11: Static force at various displacements and temperatures

4 Black Box modelling of a controllable damper

4.1 Introduction

In Section 3, a mathematical model for a passive damper was derived, based on physical laws and straightforward assumptions. To model a controllable damper, some specific details on the construction of the damper are important. This information, however, was not available. Therefore, a different approach will be used to model a controllable damper: the knowledge on damper mechanics as described in Section 3 is only used as a basis for choosing the structure of the model. The main approach is to try to fit measured damper behaviour in simple differential equations. Only known dependencies are modelled.

Figure 12 shows the basic structure of the model, consisting of four parts. Section 4.2 describes a linear, steady-state model, the interpolation model. This is based on an idea of Muijderman [18] and observations by Huisman [9]. In Section 4.3 the influence of the gas spring will be modelled, i.e. the influence of the position q on the damper force F . In Section 4.4, the dynamics in the transfer from relative velocity \dot{q} to damper force F will be dealt with. This is the oil dynamics, i.e. the dynamics resulting from compressibility of the oil and damper construction. Section 4.5 deals with the transfer from damper control voltage v to damper force F , also known as valve dynamics, i.e. dynamics induced by damper electronics and valve actuators. Several methods are described to model the valve dynamics.

In Section 4.6, the resulting second order model is compared to the model derived by Besinger *et al.*. In Section 4.7 the first order model and second order model are compared to results obtained by hardware-in-the-loop simulations. In Section 4.8 conclusions are drawn.

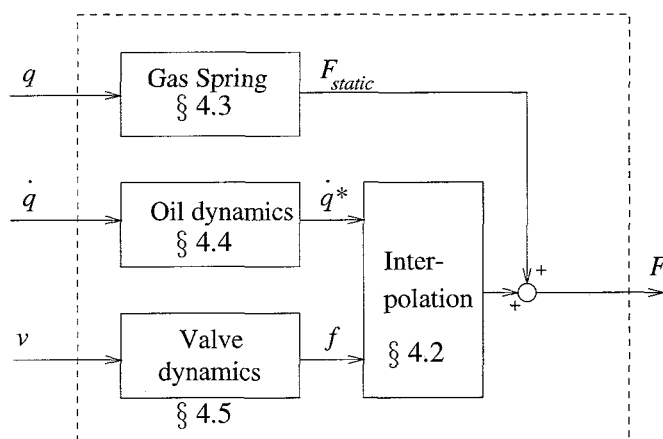


Figure 12: Simple 'Black Box'-model

4.2 Interpolation

model

The ÖHLINS damper is continuously adjustable: adjusting the control voltage to the damper electronics will result in a different damping rate. Within the damper, a servo adjusts the size of an orifice in the piston (see Figure 1).

For each velocity, the damper has a minimal setting ('soft' setting, large orifice) and a maximum setting ('hard' setting, small orifice), as seen in Figure 13.

Muijderman [19, Section 2.2] introduces a parameter f to describe the damping force as an intermediate value between the hard and the soft setting (see Figure 13):

$$F = f F_{\text{hard}}(\dot{q}) + \{1-f\} F_{\text{soft}}(\dot{q}) \quad (39)$$

When f is maintained at zero, the damper acts like a soft passive shock absorber ($F = F_{\text{soft}}(\dot{q})$), where on $f = 1$ the damper characteristic can be described as hard: $F = F_{\text{hard}}(\dot{q})$.

The value of f depends non-linearly on the control voltage v of the damper. This dependence, the valve dynamics, is discussed in Section 4.5.

Obtaining hard and soft damper curves

Two different approaches can be used to obtain the necessary hard and soft damper curves $F_{\text{hard}}(\dot{q})$ and $F_{\text{soft}}(\dot{q})$:

- The hard and soft damper curves can be obtained from the WhiteBox model using appropriate parameters for each curve. This method also incorporates temperature influences and hysteresis due to the gas compartment, as these are part of the WhiteBox model. The result would be a so-called "grey" model: both the BlackBox and WhiteBox approach would be used in one model.
- It is also possible to use measured damper curves for both settings. Huisman [9, Appendix 2] measured the damper forces of the hard and soft setting using the Constant Velocity-method. This means that at various constant velocities, the damper force is measured with the control voltage at 0.5 [V] ($\approx f = 0$) for the soft curve and at 3.235 [V] ($\approx f = 1$) for the hard curve. Measurements were taken after switching dynamics had damped out, thus at constant velocity and constant control voltage. The damper was heated in advance to its working temperature. These measurements are

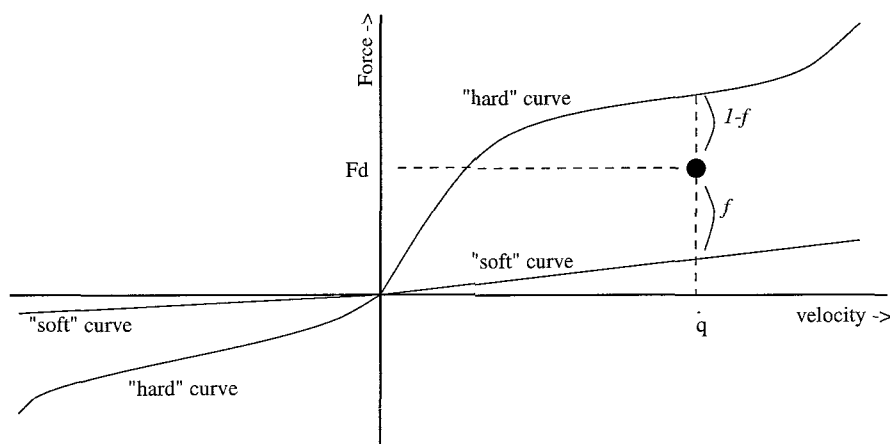


Figure 13: Interpolation between 'hard' and 'soft' curve.

used in a look-up table to provide the functions $F_{\text{hard}}(\dot{q})$ and $F_{\text{soft}}(\dot{q})$. Data obtained by the Constant Velocity method are better than the VDA-test (refer to Section 2.3.1) because less information on hysteresis is discarded this way.

The advantages and disadvantages of the use of the measured damper curves instead of the WhiteBox model are:

- + using measured data might be a good protection against model uncertainties.
- + using a look-up table is far less computation-intensive than using the WhiteBox-model. This would be a major advantage for real-time model-based controllers.
- only the force velocity-curve is used, discarding all knowledge on position dependence. (This can be partially solved by inserting a gas spring into the model, see next section).
- all knowledge on temperature-influences is lost, as the obtained damper curves are for working temperature only.

It was chosen to use the measured damper curves.

4.3 Gas spring

In the previous section, it was decided to use measured force-velocity curves. However, from the WhiteBox model it is clear that the compartment with nitrogen gas acts as a gas spring, thus introducing a position-dependence.

Section 3.5 dealt with the static damper forces, which are generated by this gas spring. It was shown that these static damper forces are non-linear and relatively small around the nominal position of the damper ($q \approx 0.2[m]$), but increase rapidly in the neighbourhood of $q \approx 0.4[m]$.

This could be modelled by an additional gas spring-block in the black box model. However, the static forces are relatively small and vary far less than the velocity does. Since the main goal of the black box model is to develop a good control algorithm⁴, this can be neglected.

4.4 Oil Dynamics

The “oil dynamics” deal with the dynamic effects which might be introduced by oil compressibility or entrapped gas in the damper oil. The effects of valve inertia and valve switching dynamics (thus valves which do not respond immediately to variations in oil flow) should also be incorporated in this section, just as velocity-dependent effects like Coulomb friction.

In the WhiteBox model, oil compressibility and valve inertia were neglected, probably resulting in inadequate modelling of hysteretic effects. However, it is unclear, how these effects should be incorporated using linear algebraic equations or linear transfer functions.

Friction was neglected due to the small influence on damper forces in heavy vehicles.

4.5 Valve Dynamics

4.5.1 Introduction

Due to dynamics in the control mechanism (a time lag?) and valve actuators, the damper does not react instantaneously to a step in the control voltage v . There will be a time delay and additional effects like overshoot might occur.

⁴For instance a the integral action of a PID-controller will take care of such “static” off-sets

The valve dynamics are modelled as a scaling with saturation and a dynamics part with first or second order dynamics. The first order dynamics will be discussed in 4.5.2, while the second order dynamics are discussed in 4.5.3.

The valve dynamics concern the transfer from the control voltage v to the damper setting f . The input to the damper is a control voltage v , ranging between 0 and 3.5 [V]. According to Huisman [9], below 0.5 [V] the damper switches to a fail-safe mode. Above 3.0 [V], the damper setting does not change if v is changed. An intermediate variable, the scaled damper control voltage v_{sc} , is introduced:

$$v_{sc}(t) = \begin{cases} 0 & \text{for } v(t) < 0.5, \\ \frac{v(t)-0.5}{2.5} & \text{for } 0.5 \leq v(t) \leq 3.0, \\ 1 & \text{for } v(t) > 3.0. \end{cases} \quad (40)$$

Note that this equation is steady state. Valve dynamics will be discussed in the next paragraphs.

4.5.2 First order valve dynamics

Muijderman [19] assumed that the dynamics of the transfer from v to f can be characterised by a first order transfer function:

$$\begin{aligned} \tau_c \dot{f} + f(t) &= v_{sc}(t) \\ \xrightarrow{\mathcal{L}} f(s) &= \frac{1}{\tau_c s + 1} v_{sc}(s) \end{aligned} \quad (41)$$

This was based on the assumption that f is influenced by v , but not by \dot{q} .

From the experiments of Huisman [9], it was concluded that a reasonable value for the first-order constant delay τ_c is $6.5 \cdot 10^{-3}$ [s].

Results

Huisman [9, Appendix 6] compares a simulation with the Muijderman model to measurements of the real ÖHLINS damper for $\dot{q} = 0.26$ [m/s]. Conclusions are drawn in [9, Section 3.2]:

*“From the responses shown in Appendix 6 we can conclude that often the simulated response deviates significantly from the measured one. The Hardware-in-the-loop experiments presented in the next chapter have to make clear whether the damper model is anyway accurately enough to predict the **vehicle response**.”*

The results of the Hardware-in-the-loop experiments are presented in [9, Section 5]:

*“With respect to the **validity of the nonlinear damper model**, it can be concluded that the damper model is not accurately enough to predict the vehicle behaviour on incidents, but it is (surprisingly) accurately enough for stochastic road surfaces.”*

Therefore, a new model will be presented in the next section to overcome most problems related to the Muijderman model.

4.5.3 Second order valve dynamics

Introduction

From the step responses in Huisman [9, Appendix 4], it is obvious that first order dynamics is only a rough approximation of the damper behaviour. In [9] the damper is excited using a set of constant

velocities, in either compression ($\dot{q} > 0$) or rebound ($\dot{q} < 0$). The damper control voltage is switched between hard (3.235 [V]), soft (0.5 [V]) and medium (2 [V]). The response of the damper force to this switching is measured. From the results, a few observations can be made:

- The dynamical behaviour varies from first order to second order with overshoot,
- A varying time lag occurs,
- The behaviour seems to depend on the sign of the change in control voltage and on the relative velocity \dot{q} ,
- The damper sometimes resonates.

To model all phenomena, second order dynamics with time lag is necessary. The resulting differential equation is:

$$\tau^2 \frac{\partial^2 f}{\partial t^2} + 2\zeta\tau \frac{\partial f}{\partial t} + f = v_{sc}\{t - t_d\} \quad (42)$$

where τ is the **natural period of oscillation**, ζ is the **damping factor** and t_d is **time delay** [23]. To model the various types of behaviour mentioned before, the parameters τ , ζ and t_d must vary. Therefore, in the next paragraph, the magnitude of these parameters will be estimated for various situations.

Estimation of the parameters

In [9, Appendix 4], the responses of an ÖHLINS shock absorber on a step in control voltage at various constant velocities are displayed.

There are a few methods to extract the desired parameters from these responses:

• **Extended Kalman-algorithm** An Extended Kalman Filter can be used to estimate the state of a system. Unknown parameters can be estimated by using an augmented state consisting of both the real state and the unknown parameters. For the model of the valve dynamics in (42), this can be done by defining the *extended state* as:

$$x^{*T} = [f, \dot{f}, \tau, \zeta, t_d] \quad (43)$$

with the scaled control voltage v_{sc} as input.

Huisman provided measurement data of the ÖHLINS damper: response of the damper force on a step in the control voltage at constant voltage. The resolution of the responses, however, was quite low, probably resulting in too few data points.

Besides, the amount of effort needed to implement the EKF to estimate all parameters using was considered too large for this simple application.

• **Least Squares approximation** Simulation of (42) using data (velocities, control voltages and forces) supplied by Huisman from tests conducted at MONROE Belgium, results in a data set of simulated damper forces $F_s(t, \tau, \zeta, t_d)$ in discrete time: (t_i, F_{s_i}) with $0 \leq i \leq n$.

The real response consists of a set of measurement data (t_i, F_i) . We can calculate the *Sum of Squares Estimator*:

$$SSE = \sum_{i=0}^n [F_i - F_{s_i}]^2. \quad (44)$$

If this SSE is minimised as a function of τ , ζ and t_d , the result is the best possible fit in sense of *Least Squares* (See Figure 14). A minimal SSE can be achieved by minimising the partial differences $\frac{\partial SSE}{\partial \tau}$, $\frac{\partial SSE}{\partial \zeta}$ and $\frac{\partial SSE}{\partial t_d}$. A minimal SSE might be achieved after several runs of the simulation process.

An analytical solution (all partial differentials equal zero) is usually impossible, but using numerical minimisation, it is possible to obtain a least squares solution. Several algorithms are available (like the ones used to train Neural Networks), but might take some time to implement. This is considered not worth the trouble at the moment.

• **Trial and Error Method** Another algorithm is to do the optimisation of the parameters by hand. By choosing parameters and running the simulation over and over again, one can estimate parameter values.

The user can calculate the SSE (equation 44) to obtain information about the “goodness of fit”. Still, the resulting parameters are only rough approximations, as humans do not have the accuracy of automated algorithms.

The results can be found in Appendix D.

Used Parameters

From the table in Appendix D, it can be seen that the obtained parameters for τ , ζ and t_d vary a lot. Therefore, three sets of parameters will be used to represent the second order model:

name	value	τ	ζ	t_d
minimal	small	0.0025	0.55	0.001
nominal	mean	0.0042	0.6267	0.0029
maximal	large	0.006	0.7	0.005

These parameters can be seen as a nominal value and an estimation of uncertainty. However, it was observed that the parameters depend on — for instance — the relative velocity and sign of the change in damper control voltage. The parameters also change fast during operation.

It is assumed that if a controller is capable of controlling all three models, it is likely that the controller is robust enough to control the real damper. However, this might be a very dangerous assumption, due to the very fast parameter changes.

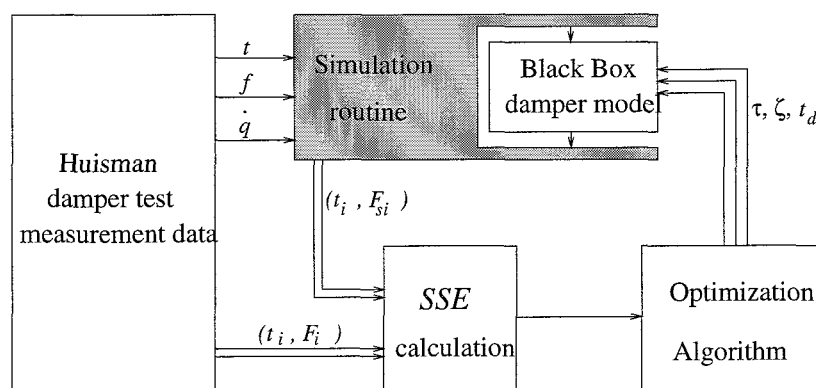


Figure 14: Schematic drawing of parameter estimation using SSE .

4.6 The second order damper model by Besinger

Another black box controllable damper model is provided by Besinger, Cebon and Cole [2]. Their damper “is provided by an European manufacturer for use in passenger cars”. No other information on the damper is given.

Their damper model (see Figure 15) is also based on second order valve dynamics. When compared to the model derived in this section, a few remarks can be made:

- They also deal with a monotube damper, as they use a “damping force offset” (i.e. a static damper force⁵),
- In Section 4.4 it turned out that the time delay from velocity input to damping force output was negligible. Besinger *et. al.* however, model a delay for the both the transfer of v to F and \dot{q} to F of 3 [ms] ,
- They use a linear damper equation

$$F = C(v) \dot{q} \quad (45)$$

for damper force calculation. This is a severe simplification, which is not acceptable for the ÖHLINS damper.

In their article, the damper is used in Hardware-In-the-Loop simulations. According to their conclusions, the results are promising... The resulting model is not further used in this report, largely because of the assumed linear characteristics.

⁵Some twin-tube dampers also have a static force, but generally the twin-tube static force is much lower

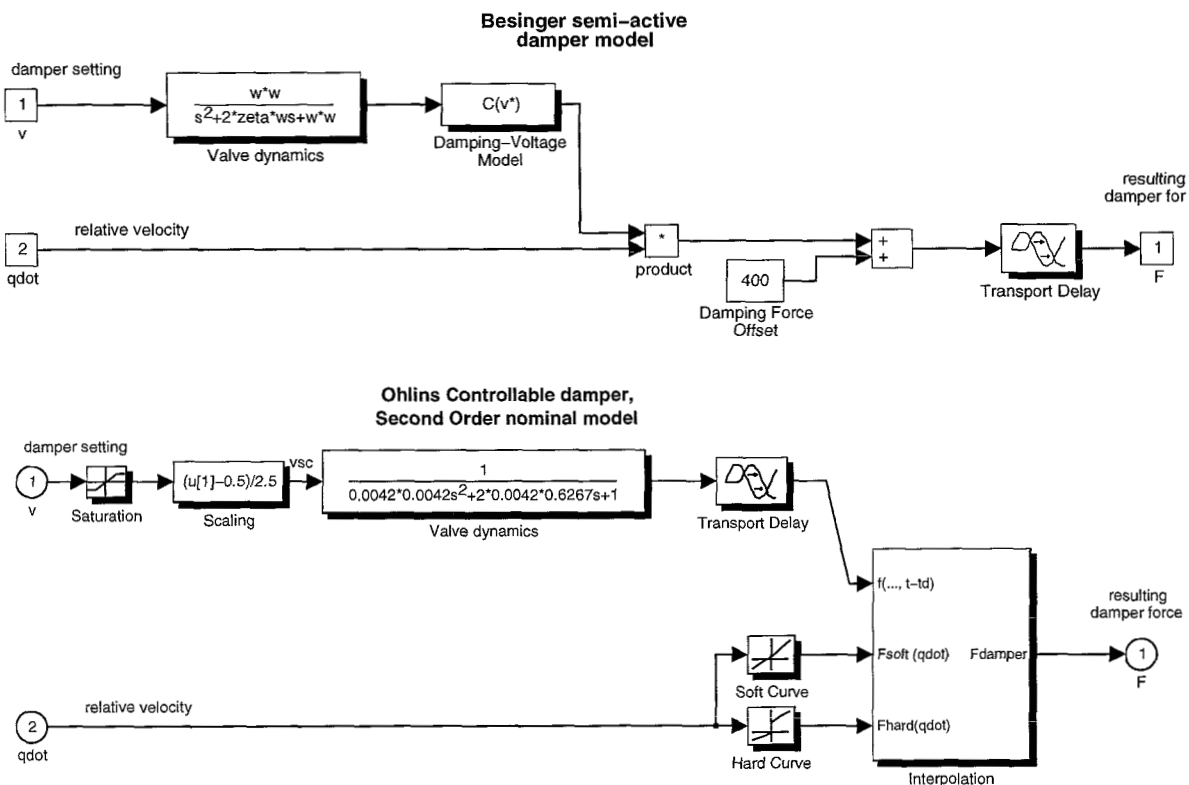


Figure 15: Comparison of Besinger model (above) and Ohlins model (below)

4.7 Performance of the first and second order damper models

Huisman [9] supplied measurement data obtained in Hardware-in-the-loop simulations with the ÖHLINS damper. This measurement data consisted of the road profiles, measured damper forces and the damper control settings. The hardware-in-the-loop simulations were done to evaluate the skyhook damping principle. In a skyhook experiment, the shock absorbers in the suspension (thus between road and chassis) are adjusted to imitate the behaviour of a damper connected to chassis and a fixed height "in the sky". See Figure 16.

Using the data from Huisman, these Hardware-in-the-loop experiments were simulated, using the damper models from this report instead of the real ÖHLINS damper. and the resulting damper forces were compared.

The road profiles used were a Traffic Hump (see Section 5.3) and a positive step [9, Section 4.3]; the skyhook damper was thought to have a setting of either $17.5[kNs/m]$ or $35[kNs/m]$. The simulation data consisted of a time vector ranging from -1 to 2 seconds. Performance evaluation is done with the time lag compensated RMS as will be described in Section 5.4.2. Results of the simulations are given in the table below:

road profile	skyhook damper setting [kNs/m]	RMS_{comp}			
		1st order	2nd minimal	2nd nominal	2nd maximum
Traffic Hump	17.5e3	618 ($n = -10$)	625 ($n = -11$)	739 ($n = -9$)	897 ($n = -8$)
Traffic Hump	35e3	548 ($n = -10$)	574 ($n = -11$)	664 ($n = -9$)	826 ($n = -7$)
Step up	17.5e3	827 ($n = -5$)	860 ($n = -6$)	801 ($n = -4$)	846 ($n = -1$)
Step up	35e3	472 ($n = -6$)	557 ($n = -7$)	620 ($n = -4$)	659 ($n = -2$)

The results show a few things:

- the RMS of the first order model is generally lower than any of the second order models. This can be explained by the nature of the second order models: each model is only valid for a specific working area of the damper, while the whole area of the damper is used.
- the test equipment contains some time lag. The damper models respond faster to velocity changes (as desired by the Hardware in-the-loop simulations) than the real model.
- the differences in time lag between the second order models are clearly visible.

As the first order model is the better general model, whilst the second order model describe extreme situations better, it is decided that all four models will be used in the next sections to serve as controllable damper model.

4.8 Conclusions

Using Black Box modelling techniques, it is possible to model the control influences of a controllable damper. It was chosen to use a real black box model, based only on measurement data. Another possibility was to use the previously derived white box model as a basis for the damper behaviour. The black box model incorporates specific damper behaviour as an look-up table, combined with a first or second order model for the valve and control dynamics.

First, control dynamics were modelled using a first order model. However, on step inputs in control voltage, the response of the ÖHLINS damper showed behaviour varying from first order behaviour to second order underdamped behaviour.

Therefore, using second order dynamics, a new damper model was fit on the various experiments. The results showed that large deviations in damper parameters occur under different circumstances.

The first order model and second order model were compared in some simulations based on hardware-in-the-loop experiments. On average, the first order model yields a better performance as it is an overall fit, while the second order models are valid for a specific working zone only. Therefore, all models will be used in the next sections.

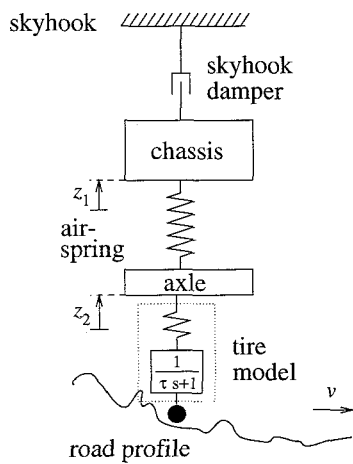


Figure 16: Skyhook damping in a quarter car model (ideal)

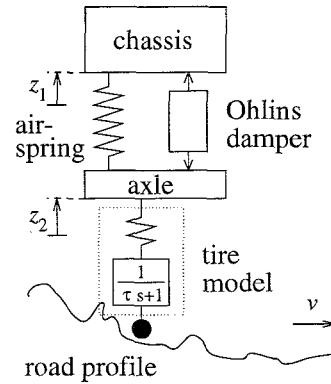


Figure 17: real world implementation of skyhook principle

5 Performance evaluation

5.1 Introduction

In order to compare various controllers on the ÖHLINS damper, some criteria must be devised to evaluate the controller performance. The general control goal is that **a test driver is not allowed to notice the difference between a passive damper and the imitation of the same passive damper by the ÖHLINS damper.**

Comparing responses of both damper forces directly (Section 5.4.2) will show that perfect tracking is impossible, there will always be an error due to time lags and unmodelled dynamics.

More important, however, is how the driver experiences these differences. To study the influence of tracking errors, a model of the truck and driver is used to estimate the influence of the errors on the senses of the driver. Section 5.2 deals with the basic structure of simulation models of a truck suspension and the connection between truck and driver. Realistic road profiles are discussed in Section 5.3.

In Section 5.4.1, the performance is evaluated from the driver's view. Section 5.4.3 contains an overview of all discussed criteria.

The resulting simulation model and the criteria will be used in the Section 6 to evaluate the chosen controllers. Please note that all results mentioned in this section are for illustration purposes only. Exact results and full simulation data will be given in the next section.

5.2 Suspension and driver model

To provide realistic excitation signals to the damper, i.e. to have a realistic relative damper velocity $\dot{q}(t)$, the truck vehicle dynamics have to be simulated. Several possible truck suspension models exist.

Muijderman [19] uses a DADS three dimensional multi-body model for simulation purposes. The model includes amongst others the tractor chassis, the cabin, the engine with transmission and front and rear suspensions. It does contain the influences of both horizontal and vertical displacements, along with the *roll* and *pitch* rotations. This model is far too complex for the purpose of this report.

Huisman [10] used a two-dimensional, four DOF⁶ model for the simulation of a truck. Only two wheels are simulated and the roll displacement is discarded. The remaining degrees of freedom are the vertical displacements of both wheels and chassis and also the jaw rotation of the chassis. A similar model is used by Isermann and Bußhardt [11] and is compared to a 1-D two DOF "Quarter Car"

⁶DOF=degrees of freedom

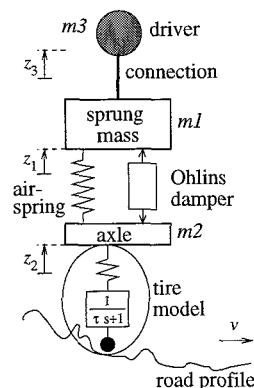


Figure 18: *Quarter car model with driver.*

model. They conclude that the only reason to use a 2-D model is the availability of the jaw rotation: the other parameters can also be taken from the 1-D model. As the influence of one damper to the chassis (sprung mass) is needed only, a quarter car⁷ model with driver is used.

The two DOF 1-D quarter car model is depicted in Figure 18. It consists of a unsprung axle mass m_2 and the sprung chassis mass m_1 , interconnected by an air spring and a damper. Explanation on the model and its parameters is done in Appendix E.

According to ISO 2631, the seated human body is especially sensitive to vertical accelerations in the frequency range between 4 and 8 [Hz] and to horizontal excitations in the frequency range up to 2 [Hz]. Most comfort measurements are related to the acceleration of the excitation [19] [30], but some investigations show the jerk (triple derivative to time) as major cause of the sensitivity.

To incorporate force exertation on the driver, the driver is modelled as a point mass of 80 [kg], connected to the sprung mass by a stiff spring and a weak damper. The stiffness of the spring is assumed to be $k = \frac{800[N]}{0.01[m]} = 80[kN/m]$ which accounts for the deformation of the chair and the body. The resulting mass-spring-damper system can be seen as a second order filter. The damping rate ζ must lie close to unity. Then $\omega_0 \approx 5[Hz]$ and the damper will have $b = 5000[Ns/m]$.

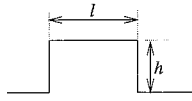
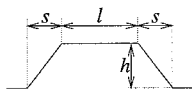
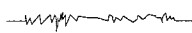
5.3 Road profiles

In many of the simulations, a road profile has to be simulated, which excites the suspension model. Muijderman [19] uses five different deterministic road profiles: *Standard Brick*, *Traffic Hump*, *Scraped Road*, *Well* and *Wave*. Only the first two profiles will be used in this report. The Standard Brick profile — a simple brick on a flat road — is a real-world implementation of the δ (Dirac)-function, whilst the Traffic Hump is a good test for the overall-performance of the suspension.

Another road profile which might be interesting is the stochastic road profile as described by Huisman and Vissers [9]. It is also known as the “DAF Bricks” road surface. The profile is created by low pass filtering of a white noise signal.

Other excitation signals, like e.g. sinusoidal excitation, *Chirp*-signals and semi-periodic signals, are not used because they do not directly relate to real-world road profiles.

The dimensions of the profiles are given in the table. Also, the forward vehicle velocity and duration of the profile are given in the table:

Description	h [m]	l [m]	s [m]	v [km/h]	$\frac{l_{tot}}{v}$ [ms]
1. Standard brick 	0.105	0.065		80	2.9
2. Traffic hump 	0.600	1.400	0.100	20	470
3. Stochastic road “DAF Bricks” 	n/a	n/a		60	n/a

⁷technically speaking, the name quarter car is incorrect for the underlying model. A truck is considered, with large differences between front and (one of the) rear axles.

Each of the selected profiles has its specific merits and demerits. This is why simulations on all three road profiles will be used in performance evaluation of the damper-controller combination.

5.4 Performance criteria

In this section, several criteria will be derived to compare the performance of the controller-damper combination to the actual passive damper. Most criteria will return a scalar value, some return a graphical representation.

In all cases, the simulations are done with the DAF 95 rear axle passive damper and some controller for the ÖHLINS controllable damper. Two ÖHLINS dampers are needed to imitate the DAF 95 damper, as the ÖHLINS damper is far softer than the DAF 95 damper [9].

The controller used is not optimal, as the results are for illustration purposes only. A more detailed discussion on the implementation of controllers can be found in Section 6.

5.4.1 Performance from the driver's view

In this section, only the influence of the damper imitation performance on vertical driver acceleration $\ddot{z}_3(t)$ is discussed. This will incorporate some of the nonlinear dynamics found between the damper and the driver. Section 5.4.2 focuses of performance evaluation of the damper forces directly.

Frequency domain

The driver acceleration can be seen as a signal containing multiple frequencies. In a power spectral density plot, the power of the signal is plotted for each frequency. This is done for the “Traffic Hump” and the “Stochastic Road” road profiles in Figures 19 and 20. The driver accelerations for both the passive damper and the controlled damper are drawn. For frequencies below 10 [Hz], the curves differ only marginally.

In Section 5.2, it was noted that a seated human body was especially sensitive to vertical accelerations with frequencies between 4 to 8 [Hz]. By weighting all frequencies with a function $W(f)$, it is possible to calculate a scalar performance norm⁸:

$$J_{\text{perf}} = \sum_{f=0}^{f_{\text{max}}} W(f) \text{PSD}(\ddot{z}_3(t)) \quad (46)$$

This approach is used by Yamashita et al. [31] to develop an H_{∞} -controller for a suspension with the goal to obtain maximum comfort. Please note that it is unclear what frequency range a test driver uses to judge over the performance of a suspension and its dampers, thus the approach of Yamashita might not work here.

Time domain

Simulations in the time domain result in large vectors with the responses to the excitation (road profile). There are several ways to obtain a characteristic value describing the vector, among which the H -norms H_2 , H_4 and H_{∞} .

⁸The power spectrum density is connected to the auto correlator by Fourier transform (Wiener-Khinchine). As the *RMS* is a special case of the auto correlator, this norm can also be written as an *RMS* of the filtered signal.

An example of an H_2 -norm is the the *Root Mean Square* RMS function:

$$\text{RMS}(\ddot{z}_3) = \left[\frac{1}{T} \int_0^T \ddot{z}_3^2(t) dt \right]^{\frac{1}{2}} \quad (47)$$

Please note that the *RMS*-theory is meaningful on stochastic inputs only. It is however chosen to apply this norm also to deterministic inputs as there is no sensible alternative.

As an example, the RMS-values have been calculated for the “Traffic Hump” and “DAF Bricks” road profiles using various damper models:

Damper Type	Traffic Hump RMS(\ddot{z}_3)	Stochastic Road RMS(\ddot{z}_3)
passive	2.52	0.540
fast controllable	2.57	0.539
slow controllable	2.58	0.545

All simulations were done over six seconds, the fast and slow damper models were defined in Section 4.5.3. The resulting RMS-values are almost equal, which was to be expected as the responses are almost equal (see Figure 21). Differences between the fast and slow controllable damper are hardly noticeable.

An RMS($\ddot{z}_3(t)$)-value is a mere indication of the quality of the whole suspension: only the intensity of the responses is taken into account. A larger value indicates more or larger accelerations and reveals no information on the frequency distribution.

According to Muijderman [19, Section 2.4.1], Griffin and Howard & Griffin recommend a so-called *Vibration Dose*, defined as:

$$\text{VD} = \left[\int_0^T \ddot{z}_3(t)^4 dt \right]^{\frac{1}{4}} \quad (48)$$

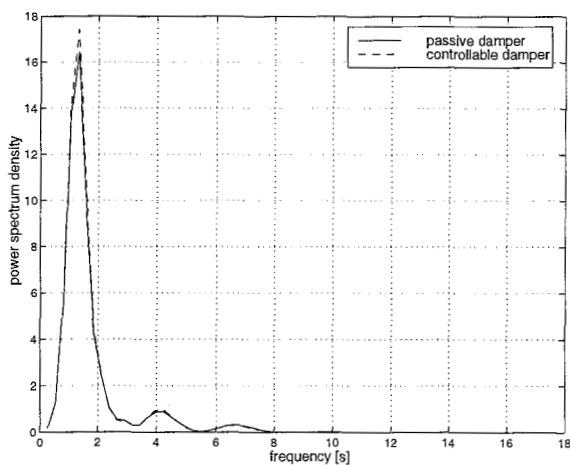


Figure 19: *Power Spectral Densities of the driver acceleration \ddot{z}_3 for the “Traffic Hump” road profile.*

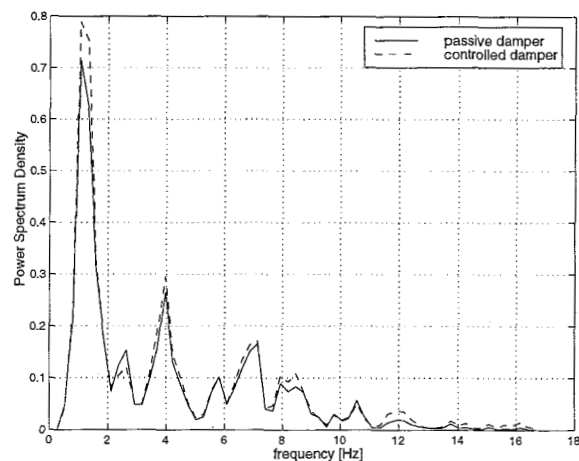


Figure 20: *Power Spectral Densities of the driver acceleration \ddot{z}_3 for the “DAF Bricks” stochastic road profile.*

This H_4 -norm warrants a stronger contribution of peak values, due to the fourth power of \ddot{z}_3 .

Muijderman [19] also uses the maximum peak value of the responses (thus a H_∞ -norm), but although this norm may contain some information on the deterministic road surfaces, this kind of norms are not used.

Difference in time domain

To compare the performance of a controlled damper to a passive damper, one could RMS the difference of both responses, like Besinger et al. [1]: They compare the characteristics of a real damper $x(t)$ with its model $y(t)$ by using an *Error Coefficient Of Variation*:

$$\text{ECOV} = \left[\frac{\int_0^T \{x(t) - y(t)\}^2 dt}{\int_0^T x(t)^2 dt} \right]^{\frac{1}{2}} \quad (49)$$

Even a small time lag between $x(t)$ and $y(t)$ results in large ECOV-values, which renders the norm useless.

To overcome the problem of large deviations due to a small time lag, we could compensate these time lags by adapting τ to minimise

$$J_{min} = \int_0^T \{x(t) - y(t - \tau)\}^2 dt \quad (50)$$

Then a difference-based RMS-value would be defined like:

$$\text{RMS}_{\text{comp}} = \left[\frac{J_{min}}{T} \right]^{\frac{1}{2}} \quad (51)$$

The results are given in the following table:

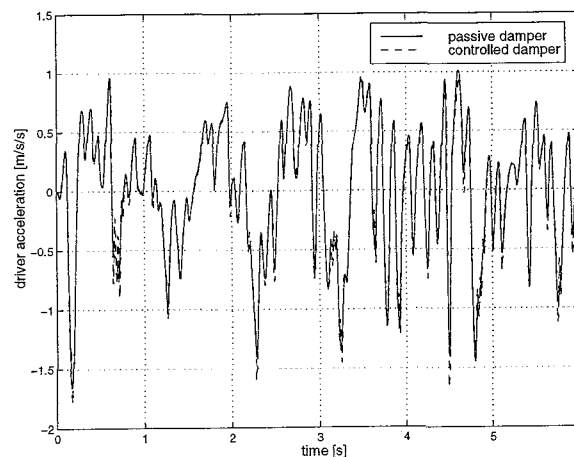


Figure 21: Comparison of the driver accelerations for a passive damper and the ÖHLINS damper imitation of the passive damper on a stochastic road profile.

Damper Type	Stochastic Road					
	$RMS_{\text{comp}}(\ddot{z}_{3,\text{con}}(t) - \ddot{z}_{3,\text{pas}}(t - \tau))$					
$\tau = \dots [ms]$	0	1	2	3	4	5
fast controllable	0.0298	0.0258	0.0323	0.0450	0.0601	0.0760
slow controllable	0.0732	0.0706	0.0724	0.0784	0.0877	0.0993

The slow controllable damper was modelled by the second order maximum model (see Section 4.5.3), with a dead time of 5 [ms], whilst the fast damper was modelled by the second order minimal model with a dead time of 1 [ms]. The non-linear vehicle dynamics and especially the low-pass filter between chassis and driver seem to trouble time lag compensation. This indicates that the time lag difference between the slow and the fast model is hardly noticeable to the driver, but note that the RMS_{comp} of the slow model exceed the fast model by two.

Equation (50) can also be used to create the time compensated $ECOV_{\text{comp}}$:

$$ECOV_{\text{comp}} = \left[\frac{J_{\text{min}}}{T \int_0^T x(t)^2 dt} \right]^{\frac{1}{2}} \quad (52)$$

The latter norm has another advantage: it is of dimension [-], which is not true for e.g. (48) and (51).

5.4.2 Performance from the damper's view

The previous section dealt with the effects of the damper imitation as sensed by the test driver. However, if the damper imitation is perfect, no differences can be felt at all. For small imperfections, the influence of the perturbations on the vehicle dynamics will be negligible. Therefore, if we assure that the errors are small, it is possible to compare damper behaviour directly without violating the performance goal from Section 5.1.

Note that allowing larger errors will lead to wrong results.

Frequency domain

Like Section 5.4.1, it is also possible to create power spectrum density plots for the damper force. A major difference between a PSD of the damper force and a PSD of the driver acceleration is the presence of an additional peak with a frequency around 10 [Hz]: the eigenfrequency of the unsprung mass. This eigenfrequency is damped out in the sprung mass to driver connection. Therefore it is absent in the PSD of the driver acceleration.

As there is no link to the driver, it is not possible to use a sensible weighting function to evaluate the power spectrum. It is however possible to evaluate the PSD and the differences on sight.

Time domain and difference in time domain

In analogy to Section 5.4.1 and 5.4.1, an RMS-based norm can be derived for the damper force $F(t)$ and the (time lag-compensated) difference between the damper force $F(t)$ and the desired damper force $F_d(t)$. The simulations were done using both a slow and a fast model for the controllable damper. The Traffic Hump road was simulated over six seconds (containing two humps) whilst the stochastic road was simulated over sixty seconds. The results are displayed in the following table:

Damper Type		Traffic Hump RMS(...)	Stochastic Road RMS(...)
passive damper force F_{des}		2.50e3	2.09e3
fast controllable damper force F		2.49e3	2.02e3
slow controllable damper force F		2.49e3	2.09e3
Fast	difference ($F - F_{des}$)	162	199
	time lag compensated difference $F(t) - F_{des}(t - \tau)$ ($\tau = 2[ms]$)	145 ($\tau = 2[ms]$)	175 ($\tau = 1[ms]$)
Slow	difference ($F - F_{des}$)	358	724
	time lag compensated difference $F(t) - F_{des}(t - \tau)$ ($\tau = 3[ms]$)	337 ($\tau = 3[ms]$)	667 ($\tau = 3[ms]$)

As one can see, the RMS -values (and especially the difference RMS -values) are very descriptive. The slow damper model should have a worse response than the fast damper and the RMS on a stochastic road should be more descriptive than the RMS of a deterministic road, like the hump. Both expectations are fulfilled.

Comparison in force-velocity plots

It is possible to calculate the relative damper velocity \dot{q} from simulations or experiments and use this relative velocity to plot force-velocity curves of the realised damper force (see Section 2.2.2). Such force-velocity curve is drawn in Figure 22, together with the maximum and minimal damper forces and the desired characteristics. In this figure, a dot is plotted at each time step of 1 millisecond.

Large deviations of the desired characteristic consume very little time, thus the influence of these errors should be quite small. It is, however, of importance to estimate this influence, as it is a measure for the performance of the controller. Therefore, a “windowed progressive averaging” is introduced. For each velocity and its n neighbouring values (a window), the mean and the standard deviation are calculated.

Assume we have a velocity data vector $qdot$ and the corresponding damper force data vector F . In MATLAB-code, the algorithm to calculate the windowed progressive averaging is:

```
function [m,s] = progressiveaveraging(qdot, F, n);
[qdotSort, I] = sort(qdot);
Fsort          = F(I);

for i = n+1 : length(qdot)-n,
    m(i) = average(i-n : i+n);
    s(i) =      std(i-n : i+n);
end;
```

In a more natural way of speaking: The velocity data vector and the damper force data vector are sorted on velocity, then a window of size $2n + 1$ moves over the sorted damper force data and the mean and standard deviation of each window are calculated.

The result is plotted in Figure 23. As can be seen, the spread of the data is relatively small. Larger deviations indicate that high damper accelerations have occurred. These accelerations are a result of the road profile. This means that comparisons between various types of road profiles are impossible.

5.4.3 Discussion

In the previous sections, several methods have been described to obtain norms for controller performance evaluation. These were separated in two groups: the drivers view, based upon the sensitivity of the driver and the damper view, based upon the responses of the damper.

Driver

Norms based upon the vertical acceleration of the driver. The merits and demerits of these norms are:

- + direct relation to the performance goal
- influence of unmodelled vehicle dynamics is unknown.
- sensitivity test driver is unknown.

The following norms were developed:

- **Frequency domain** A weighting of the PowerSpectrumDensity, based upon the sensitivity of drivers according to ISO 2631.
 - + also useful in H_∞ -controllers.
 - + visual representation of PSD is useful.
 - the uncertainty about the sensitivity of the test driver makes a plausible weighting function unavailable.
- **Time domain** The RMS of the response of the vertical driver acceleration.
 - + easy to calculate.
 - less useful for deterministic roads.
 - RMS values are a better norm to evaluate suspension comfort than to compare characteristics.
 - comparison only possible on same road profile.

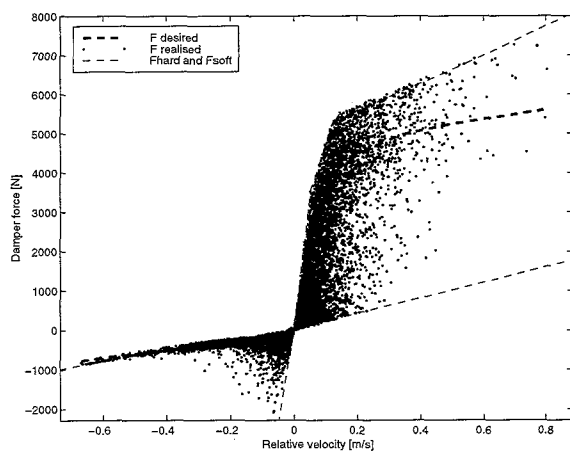


Figure 22: Force-velocity curve of the controllable damper on the “Stochastic Road” profile. Each time step of 5 milliseconds is represented by a dot. The resulting figure shows that huge deviations last rather short.

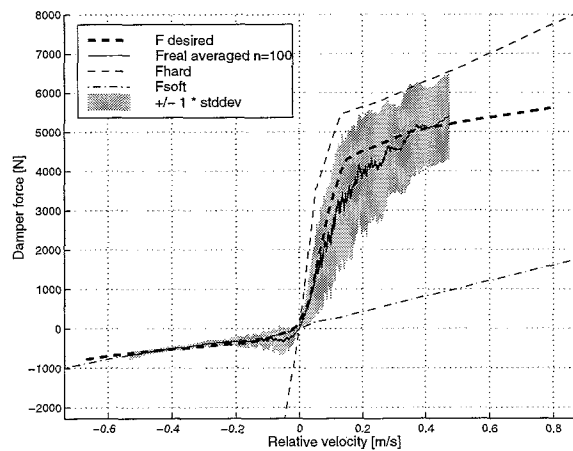


Figure 23: Force-velocity curve of the controllable damper on the “Stochastic Road” profile. The same data was used as in Figure 22, but the data was windowed and the mean and standard deviation are shown. Width of the window was 101 measurement points.

- **Time domain** The time lag-compensated RMS of the difference of two responses.
 - + easy comparison between two characteristics on the same road profile.
 - less useful for deterministic roads.
 - optimisation using time lag-compensation is dangerous as the influence of a dead time is neglected.

Damper

In case the damper forces show a little difference only, the change in vehicle dynamics will be negligible. In that case, it is possible to compare the damper forces directly.

- + easier to measure or calculate.
- + no influences from driver sensitivities.
- only useful for small differences between desired and realised damper forces.

The following norms were described:

- **Frequency domain** A weighting of the PowerSpectrumDensity, based upon the sensitivity of drivers according to ISO 2631.
 - + visual representation of PSD is useful.
 - only a visual norm is available.

- **Time domain** The RMS of the damper force response.
 - RMS leads to interesting results for stochastic roads only.
 - results only comparable on same road profile.

- **Time domain** A plot of the responses of the realised and desired damper forces.
 - + easy comparison by viewing the responses.
 - + contains all necessary information, but for trained eyes only.
 - only visible criteria possible.

- **Time domain** The time lag-compensated RMS of the difference of the passive damper response and the controllable damper response.
 - + easy comparison between damper behaviour possible.
 - RMS leads to interesting results for stochastic roads only.
 - results are not comparable between road types.

- **Force-velocity curve** A plot consisting of the “windowed progressive mean” and the standard deviation of the controllable damper characteristics.
 - + Very clear and intuitive to use.
 - + Reliable results on both deterministic and stochastic road profiles.
 - It is only a visual norm.
 - Norm is sensitive to damper accelerations, which makes comparisons between different road types impossible.

It is chosen to use the damper responses as these are relatively well-documented and without the uncertainties of the driver objectives and sensitivities:

- time lag-compensated RMS .
- graphical representation of “windowed progressive mean” and standard deviation.
- time response plot of the realised and desired damper forces.

5.5 Conclusions

The difference between a passive damper and the imitation of the same passive damper by an controllable damper is not allowed to be noticed by a test driver. As there inevitably will be differences in desired and realised damper force, the impact of the differences on the driver must be established. Due to large uncertainties in truck and driver modelling, it was not possible to obtain an undisputable norm.

Several methods were described to compare the desired behaviour of the damper with the realised responses directly. It was chosen to use a time lag compensated *RMS*-based criterium and some graphical representation of the realised force-velocity curve, called the windowed progressive average.

6 Controller

6.1 Introduction and control objective

The main objective of this report was to develop a controller for the ÖHLINS controllable damper, which allows test drivers to enter a certain passive damper curve, which then is imitated. This will greatly reduce development time of a truck suspension, as it is no longer necessary to replace passive dampers during test driving procedures.

The control objective can then be written as:

“Have the controllable damper follow a prescribed passive damper curve as closely as possible.”

In Section 6.2, the controlled system is defined, identifying in- and outputs. Section 6.3 deals with the basics and the tuning of PID-controllers. Section 6.4 discusses the results obtained by the PID-controller. Section 6.6 discusses some improvements to the current controller, whilst Section 6.7 mentions some other controllers which might yield better performance. Finally, Section 6.8 draws conclusions.

6.2 System definition

In order to be able to design a controller, the system which is to be controlled must be defined clearly. In this case, it means: draw a fence around the object, and mark all interactions through the fence as inputs, outputs and disturbances.

In our case the object is a passive damper (see Figure 24 within the fence) with an input: the relative velocity \dot{q} and an output: the resulting damper force $F(t)$.

This passive damper is replaced by an ÖHLINS controllable damper, as drawn in Figure 25. It can be seen that one extra input is added: the control voltage v , which is used to set the damping. The relative velocity \dot{q} and the damper force need to be measured. Measuring of these signals is assumed to be perfect and is not further discussed here. For simulation purposes, the ÖHLINS damper is replaced by its second order nominal model, as derived in Section 4. The interpolation model of Section 4.2

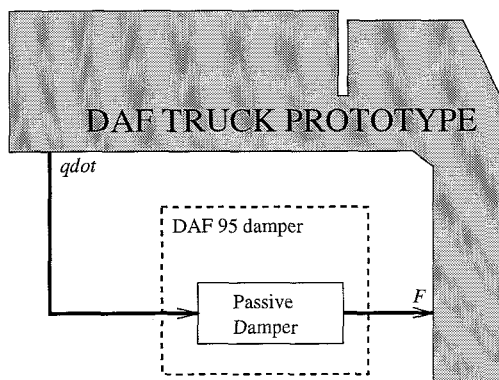


Figure 24: Damper in Truck: inputs and outputs.

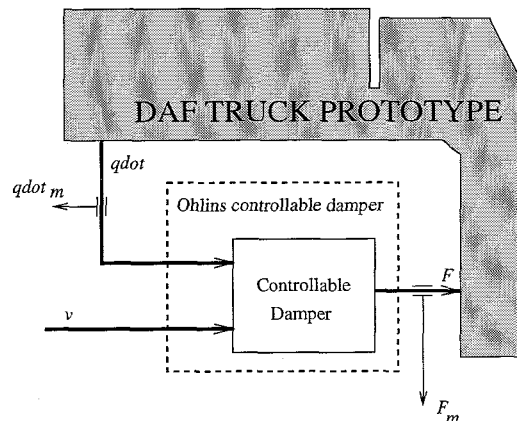


Figure 25: The replacement of the passive damper by an ÖHLINS controllable damper and the definition of (measured) in- and outputs.

(The *IP*-block in Figures 26 and 27) is independent of the internal damper dynamics. This means that a correct setting of f will always result in the expected damper force. If all model errors are assumed to be disturbances of the valve dynamics, all dynamics are contained within the transfer from the damper control voltage v to the internal damper setting f . Then the internal damper setting f would be the feedback signal. This is drawn in Figure 26. The controller is a “Tracking” controller, which tries to maintain the tracking error $\epsilon = f_d - f$ at zero. The desired damper force $F_d(\dot{q})$ characteristic is known. the desired internal damper setting $f_d(\dot{q})$ is calculated by applying equation (39):

$$f_d(\dot{q}) = \frac{F_d(\dot{q}) - F_{\text{soft}}(\dot{q})}{F_{\text{hard}}(\dot{q}) - F_{\text{soft}}(\dot{q})} \quad (53)$$

Unfortunately, f is not measured. Therefore, it has to be calculated from the resulting damper force F in analogy to (53). The tracking error ϵ can then be written as:

$$\epsilon(\dot{q}) = f_d(\dot{q}) - f(\dot{q}) = \frac{F_d(\dot{q}) - F(\dot{q})}{F_{\text{hard}}(\dot{q}) - F_{\text{soft}}(\dot{q})} \quad (54)$$

The resulting control configuration is drawn in Figure 27. Note that the fraction $\frac{1}{F_h - F_s}$ is not straightforward to implement, due to the step from $-\infty$ to $+\infty$ at zero velocity.

6.3 PID Controller

As a first controller, a commonly used PID-controller is used. In the Laplace domain, this controller is defined by:

$$C(s) = K_p \left\{ 1 + sK_d + \frac{1}{sK_i} \right\} \quad (55)$$

This controller was tuned using the second order nominal model from Section 4.5.3. To obtain a first estimation on the proportional, integral and differential parameters K_p , K_i and K_d , a Ziegler-Nichols tunings method is used [7, p. 103] [23, p. 352]. This algorithm may be used if and only if the plant is at least underdamped and overshoot is allowed. Both conditions are met in this case. The procedure

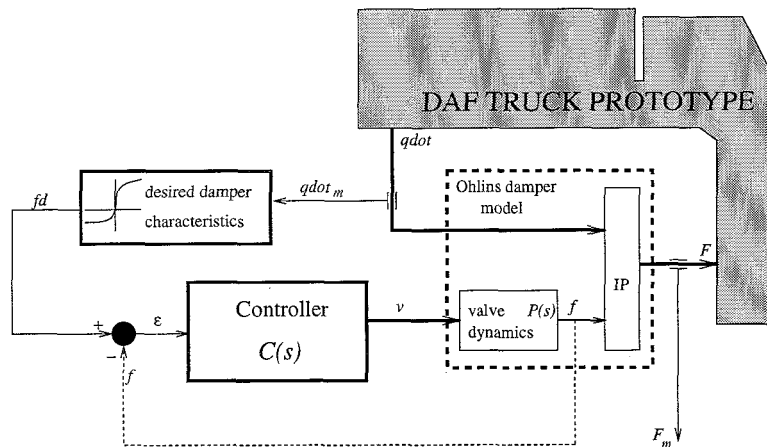


Figure 26: The desired control configuration, using feedback of the internal damper setting f .

starts with the increase of the closed-loop gain g_0 until undamped oscillations occur with period T_0 . Then the K_p , K_i and K_d are defined:

$$K_p = 0.60 g_0 \quad K_i = 0.50 T_0 \quad K_d = 0.125 T_0$$

Optimising the controller on a stochastic road profile, using the time lag compensated RMS, an optimal controller was found for:

$$K_p = 0.60 g_0 \quad K_i = 0.35 T_0 \quad K_d = 0.220 T_0$$

This controller yields a 20% better RMS_{comp} of the damper force performance on the "DAF Bricks" stochastic road profile than the Ziegler-Nichols tuned controller.

6.4 Results

In accordance with Section 5, the performance of the controller is evaluated using plots of the damper force response, time lag compensated RMS and using a graphical representation of the windowed progressive average.

The PID controller was tested on all four BlackBox damper models (Section 4.5.3) on different road profiles (Section 5.3). The standard brick and traffic hump road profiles were simulated, both having two road irregularities within 0 to 8 seconds. The stochastic road profile was simulated over 60 seconds. All simulations were done using a fixed step Runge-Kutta integration routine in SIMULINK 2.1.

Damper force response plots

Fragments of the damper force responses are drawn in Figures 28, 30 and 32 for the second order minimum model and Figures 29, 31 and 33 for the second order maximum model.

As one can see, the minimum model clearly follows the desired behaviour better than the maximum model. The maximum model seems to suffer from small instabilities. This is not caused by the integration scheme, it also shows using variable step integration. Probably, the controller is not robust enough.

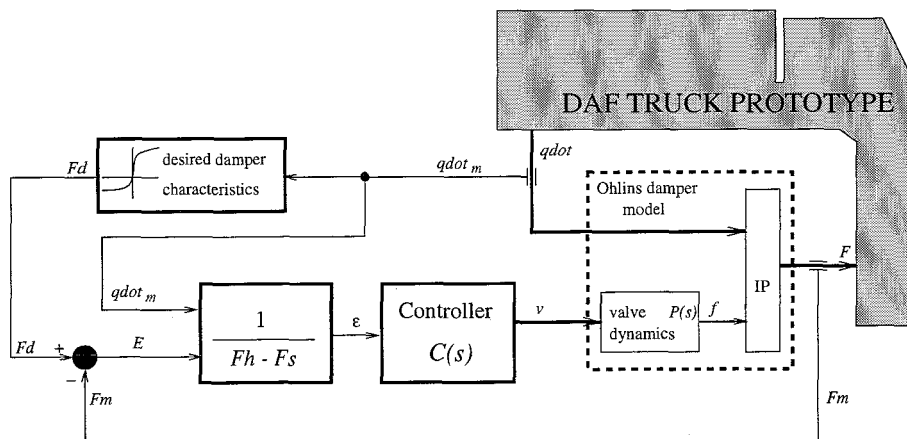


Figure 27: The real control configuration, using the damper force as feedback.

In both deterministic road profiles, it can be seen that serious deviations from the real damper behaviour occur. Especially the dip in desired damper force at $t = 1[s]$ on the standard brick road surface is disturbing.

Time lag compensated RMS

The time lag compensated RMS-values are given in the table below.

Road Profiles	RMS($F_d(t)$) passive	RMS($F(t) - F_d(t - n * 0.001[s])$)			
		1st order	2nd minimal	2nd nominal	2nd maximum
Standard Brick	8.11e2	162 ($n = 0$)	129 ($n = 1$)	184 ($n = 1$)	333 ($n = 1$)
Traffic Hump	2.18e3	136 ($n = 2$)	124 ($n = 2$)	145 ($n = 2$)	311 ($n = 2$)
Stochastic Road	2.09e3	234 ($n = 1$)	177 ($n = 1$)	266 ($n = 2$)	711 ($n = 3$)
Stochastic Road (Z-N tuning only)	2.09e3	290 ($n = 2$)	221 ($n = 1$)	290 ($n = 2$)	665 ($n = 3$)

The results benefit greatly from the extra tuning on top of the Ziegler-Nichols tuning, except the maximum second order model: the new controller results in an temporarily unstable system. Therefore, its *RMS* is higher than the more conservative tuned Ziegler-Nichols controller.

The damper has a worse performance on the second order maximum model than the other three models. Both the *RMS* and the time lag compensation strongly increase. Behaviour similar to the maximum model is shown by the real controllable damper on low relative velocities.

Windowed average

The windowed average as proposed in Section 5.4.2 is used on the data from Figure 34, a force-velocity representation of the second order maximum damper model. The results can be found in Figure 35.

Figures 36, 37, 38 and 39 show the windowed averages for the Standard Brick, Traffic Hump and DAF Bricks road profiles. The latter is shown for both the optimal tuning and the Ziegler-Nichols tuning. In each figure, the minimal and maximum second order damper model responses are drawn.

Apparently, in all cases the minimal (fast) model yields a better performance than the maximum (slow) model.

6.5 Overshoot

On a velocity sign change, the damper force has “overshoot”, i.e. when changing velocity sign to positive, the damper is still in its soft setting, thus yielding a low force. When changing to negative velocities, the damper force is too high. Note that the plots are made for the slowest damper model. Faster models show less overshoot.

During the tuning of the controller, it was observed that increase of the rate feedback K_d yields improvement for the Traffic Hump road profile. This is caused by the fact that velocity sign changes usually occur with large accelerations. By increasing the rate feedback, the controller acts stronger on large accelerations.

It was also observed that the Stochastic road profile did not improve much on the increased K_d . Decrease of the integral feedback K_i did show improvements.

The final controller is still incapable of preventing overshoot. Increasing the bandwidth of the damper, i.e. making the controllable damper faster will solve the problem.

6.6 Improvements

In this section, several extensions of the PID-controller are discussed to improve the control performance.

Dead time compensator

The second order damper model contains a time delay, varying between 1 [ms] and 21 [ms] (see Appendix D). As an improvement over the standard PID-controller, it is tried to compensate this dead time using a Smith-predictor [23, Chapter 19]. The Smith-predictor theory splits the process (“plant”) in two parts: a block with all dynamics and a block containing the time delay. By incorporating an extra local loop around the controller, the closed-loop transfer function is altered in such way that it moves the time delay outside the main closed loop transfer.

Unfortunately, the Smith-predictor is based on linear process dynamics. However, the damper model contains a non-linear saturation function, which proved sufficient to wreck predictor-performance.

Overshoot compensator

In the real controllable damper, the performance deteriorates within the neighbourhood of zero velocity. It is assumed that this is caused by the reduction of the oil pressure, which is the driving force behind the opening and closing of the valves. Adjusting the valve settings for relative velocities below approx 0.1[m/s] is not very useful and only introduces slow dynamics [9, Section 4.3].

An approach to overcome this problem is to set the damper control voltage to maximum when entering the low velocity region with a large positive acceleration and to minimum when entering the region with a large negative acceleration, thus introducing a no-activity zone.

This approach has some similarities to a rate feedback (D -controller), but for a specific working area.

The approach was not tested with the final controller. Testing with an early version of the current control configuration showed an increase of dynamics on leaving the no-activity zone, due to the switching of the control voltage from maximum or minimum to the current value.

6.7 Other controller types

Although the PID-controller is the most widespread controller, it usually is not the controller with the best performance. This section discusses some other, more advanced, controller types which might prove better.

Feedback linearization and sliding mode controllers

The model of the continuously adjustable ÖHLINS damper as derived in Section 4 is nonlinear. However, most controller design methods lend themselves more easily for linear systems.

Feedback linearization is a method to transform nonlinear systems into linear systems (see e.g. Slotine and Li [22]). Then, the remaining linear system can be controlled using robust controllers.

A major drawback of feedback linearization is that all states have to be known. In this continuously adjustable damper case, the internal damper setting f is an unknown state. In this case, it can be *calculated* from the resulting damper force using equation 53, another possibility was to use an Extended Kalman Filter to *estimate* the f .

Some effort was made to develop a feedback linearization, based on the black box damper model. The resulting linear system was controlled using a sliding mode controller. As the blackbox model

contains huge parameter uncertainties, the effect of the feedback linearization was somewhat less than expected.

It was decided to abandon the feedback linearization approach, therefore it is not discussed further in this thesis.

H_∞ -controller

A totally different approach is the H_∞ -controller, based on frequency domain analysis. The general idea is that within a control system, different transfer functions (e.g. disturbance to error, controlled input to output) have different demands on transfer gain at different frequencies. Weighting functions are applied to the input and output signals to quantify the desired performance in each region of the frequency domain.

In the underlying case, the sensitivity of the driver is maximal for the 1 to 8 [Hz] frequency range. The tracking error $F_d - F$ must be close to zero within this range, but is allowed to be larger for other frequencies. Disturbances are known to have frequencies around 1 [Hz] (the chassis) and approx 10 [Hz] for the unsprung masses.

The H_∞ -algorithm optimises the controller, using the weighted information. Detailed information on the choice of weighting functions and performance outputs for active suspensions can be found in e.g. Yamashita et al. [31]. The application of H_∞ was not researched for this thesis.

6.8 Conclusions

It is possible to use a PID-controller to control the ÖHLINS controllable damper. The resulting control configuration was tested using simulations on three different road profiles with four different models for the controllable damper. For low relative velocities, the controller is lacking performance.

The impact of the errors induced by the low performance of the controller on the test driver's senses is still unknown, therefore it is unknown whether the controller suffices.

Several improvements are suggested, among the migration to different controller types like feedback linearization and H_∞ -control.

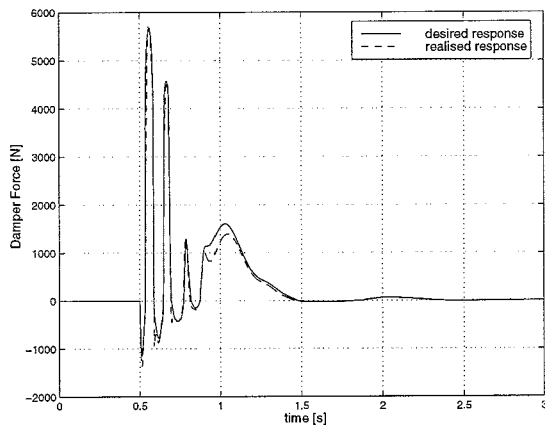


Figure 28: Time domain representation of desired and realised damper force of second order minimum model on standard brick road profile.

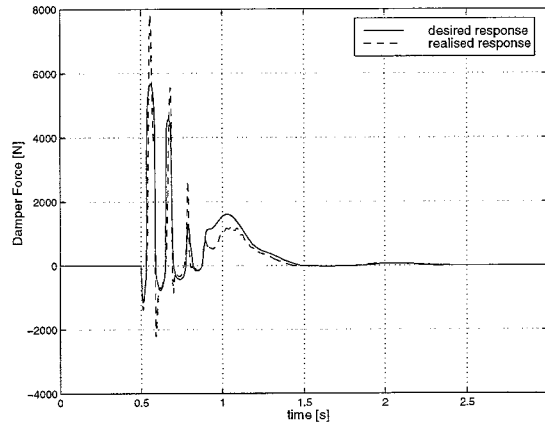


Figure 29: Time domain representation of desired and realised damper force of second order maximum model on standard brick road profile.

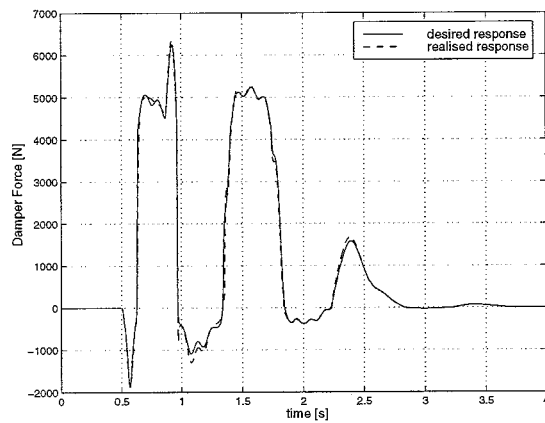


Figure 30: Time domain representation of desired and realised damper force of second order minimum model on Traffic Hump road profile.

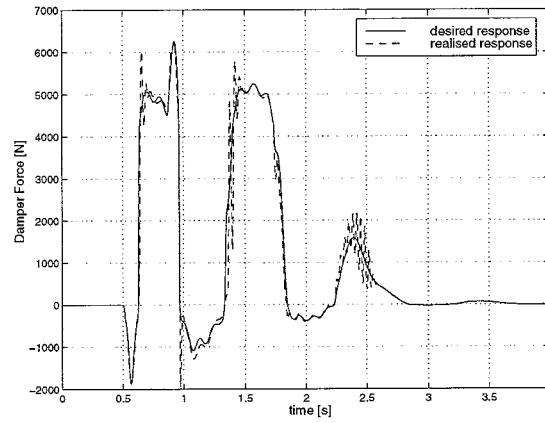


Figure 31: Time domain representation of desired and realised damper force of second order maximum model on Traffic Hump road profile.

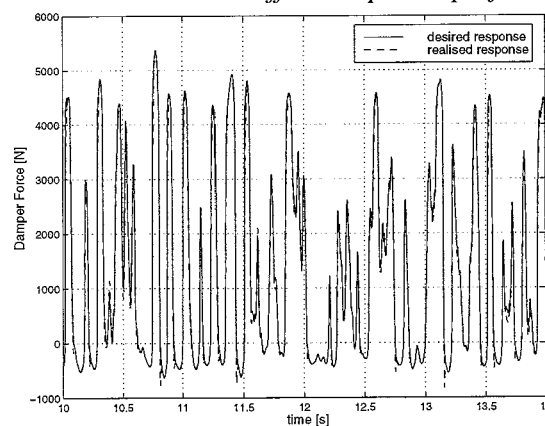


Figure 32: Time domain representation of desired and realised damper force of second order minimum model on DAF Bricks road profile.

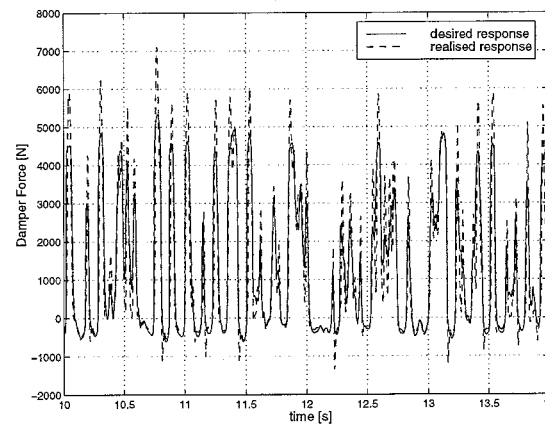


Figure 33: Time domain representation of desired and realised damper force of second order maximum model on DAF Bricks road profile.

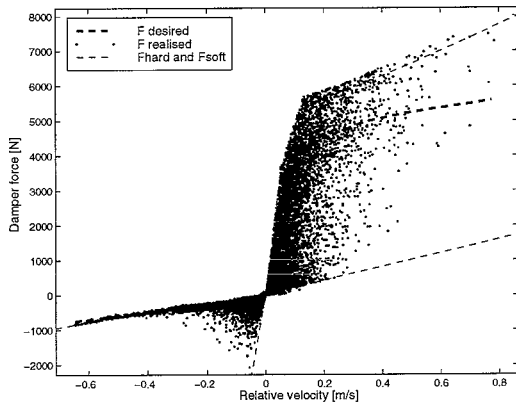


Figure 34: Force-velocity curve of the DAF Brick road surface with the second order maximum damper model. Each time step of 5 [ms] is dotted.

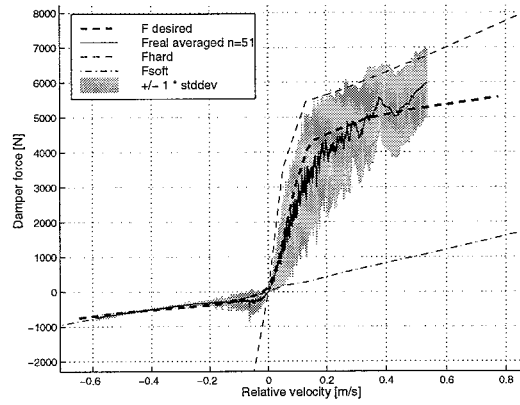


Figure 35: Force-velocity curve of the DAF Brick road surface with the second order maximum damper model. Same figure as 34, but now the window progressive averaging is used. Both the mean and the standard deviation are plotted.

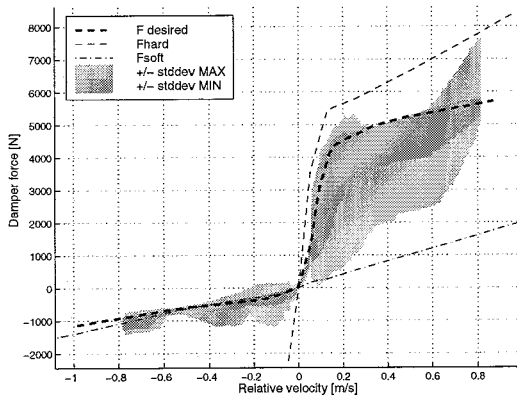


Figure 36: Windowed progressive averaging on the Standard Bricks road. Comparison between 2nd order minimum and maximum model responses.

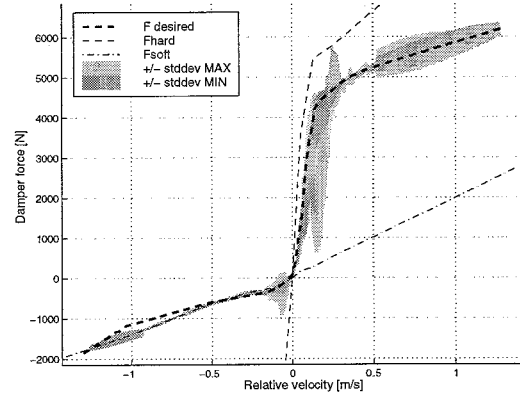


Figure 37: Windowed progressive averaging on the Traffic Hump road. Comparison between 2nd order minimum and maximum model responses.

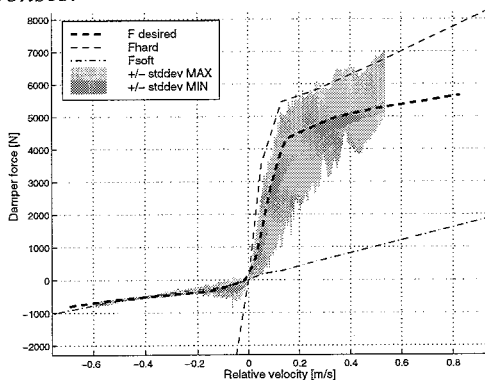


Figure 38: Windowed progressive averaging on the DAF Bricks road. Comparison between 2nd order minimum and maximum model responses.

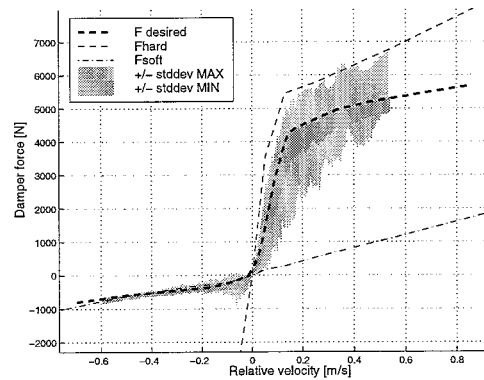


Figure 39: Windowed progressive averaging on the DAF Bricks road. Comparison between 2nd order minimum and maximum model responses, with Ziegler-Nichols tuning only.

7 Conclusions and Recommendations

7.1 Conclusions

Three kinds of graphs are commonly used to describe damper behaviour: force-velocity, force-displacement and force-velocity-displacement (Restoring Force Surface, 3D-figure). To obtain these curves, several types of experiments for parameter identification can be used. In most cases, the advantages or disadvantages break down to one simple conclusion: parameter identification is severely troubled by damper warming and non-linearities. Most characterisation methods discard much of the gained information in order to create one of the graphs mentioned above, as they measure velocity indirectly.

Two different damper models were derived: a “white” passive damper model and a “black” controllable damper model.

The white model incorporates some influence of temperature on damper behaviour. Some non-linear damper characteristics might be partially explained using this model.

To model a controllable damper, black box modelling techniques were used. It was chosen to use a real black box model, based on measurement data only by incorporating specific damper behaviour as an look-up table. Valve and control dynamics were fitted on first or second order models. Fitting of these models on step inputs in control voltage, the response of the ÖHLINS damper showed behaviour varying from first order behaviour to second order underdamped behaviour. Large deviations in damper parameters occur under different circumstances.

The first order model and second order model were compared in some simulations based on hardware-in-the-loop experiments. On average, the first order model yields a better performance as it is an overall fit, while the second order models are valid for a specific working zone only.

The difference between a passive damper and the imitation of the same passive damper by a controllable damper is not allowed to be noticed by a test driver. As there will inevitably be differences in desired and realised damper force, the impact of the differences on the driver must be established. Due to large uncertainties in truck and driver modelling, it was not possible to obtain an undisputable norm for the driver’s sensing. Therefore, only norms based on differences between desired and realised damper behaviour were used.

Several methods were described to compare the desired behaviour of the damper with the realised responses directly. It was chosen to use a time lag compensated *RMS*-based criterium and some graphical representation of the realised force-velocity curve, called the windowed progressive average. It is possible to use a PID-controller to control the ÖHLINS controllable damper. The resulting control configuration was tested using simulations on three different road profiles with four different models for the controllable damper. For low relative velocities, the controller is lacking performance.

As a results of the chosen performance tests, the impact of the errors test driver’s senses is still unknown. Therefore it is unknown whether the controller suffices.

7.2 Recommendations

The behaviour of passive shock absorbers cannot be described accurately by a force-velocity curve only. A Restoring Force Surface seems to be a good alternative. Implementation of an RFS plot as desired damper force in the current control scheme will consume a lot of time.

Using the constant-velocity method, it is possible to create force-velocity curves at various temperatures. This would benefit both the damper model and the recovery of the damper setting f from the measured damper force F .

Knowledge on the sensitivity of test drivers is lacking. The only way to obtain this information is experimenting with real vehicles. This will also answer a few other questions, e.g. whether the current PID-controller suffices.

Implementation of an H_∞ -controller might improve the performance. An H_∞ -controller is frequency-dependent, and might use a stronger gain on lower frequencies (to prevent overshoot).

References

- [1] F.H. Besinger, D. Cebon, and D.J.Cole. Damper models for heavyvehicle ride dynamics. *Vehicle System Dynamics*, 24:35–64, 1995.
- [2] F.H. Besinger, D. Cebon, and D.J.Cole. Force control of a semi-active damper. *Vehicle System Dynamics*, 24:695–723, 1995.
- [3] S. Cafferty, K. Worden, and G.Tomlinson. Characterization of automotive shock absorbers using random excitation. *Proceedings of the Institution of Mechanical Engineers, Part D*, pages 239–248, 1995.
- [4] S. Duym. An alternative force state map for shock absorbers. *Proceedings of the Institution of Mechanical Engineers, Part D*, pages 175–179, 1997.
- [5] S. Duym, R. Stiens, G. Baron, and K. Reybrouck. Physical modeling of the hysteretic behaviour of automotive shock absorbers. Technical Report 970101, SAE, 1997.
- [6] W. Foag. *Regelungstechnische Konzeption einer aktiven PKW-Federung mit "Preview"*, volume Fortsch.-Ber. VDI Reihe 12 Nr. 139. VDI-Verlag, Düsseldorf, Germany, 1990.
- [7] G. F. Franklin, J. David Powell, and A. Emami-Naeini. *Feedback Control of Dynamic Systems*. Addison-Wesley Publishing Company, Inc., Reading, Massachusetts, USA, june 1988 (reprint with corrections) edition, 1986.
- [8] P. Hagedorn and J. Wallaschek. On equivalent harmonic and stochastic linearization for nonlinear shock-absorbers. In *IUTAM Symposium on Nonlinear Stochastic Dynamic Engineering Systems*, Berlin, Germany, 1988.
- [9] R. Huisman and J. Vissers. Results of the laboratory tests with the cascov fast controllable shock absorber. Technical Report CASCOV Milestone Report no. 9, Monroe, Belgium, 1996.
- [10] R.G.M. Huisman. *A controller and observer for active suspensions with preview*. PhD thesis, Eindhoven University of Technology, Eindhoven, The Netherlands, 1994.
- [11] R. Isermann and J. Bußhardt. Selbsteinstellende Radaufhängung. *Automatisierungstechnik*, 44:351–358, 7 1997.
- [12] W.S. Janna. *Engineering Heat Transfer, (SI Edition prepared by Morgan Heikal)*. Van Nostrand Reinhold (International) Co. Ltd., London, UK, 1988.
- [13] K.M.Captain, A.B.Boghani, and D.N.Wormley. Analytical tire models for dynamic vehicle simulation. *Vehicle System Dynamics*, 8:1–32, 1979.
- [14] H.H. Lang. *A study of the characteristics of automotive hydraulic dampers at high stroking frequencies*. PhD thesis, University of Michigan, Michigan USA,, 1977.
- [15] K. Lee. Numerical modelling for the hydraulic performance prediction of automotive monotube dampers. *Vehicle System Dynamics*, 28:25–39, 1997.
- [16] M. Mitschke and K.-O. Riesenberger. Stoßdämpfererwärmung und Dämpferwirkung. *Automobil-technische Zeitschrift*, pages 133–139, April 1972.

- [17] Ch. Morris, editor. *Academic Press Dictionary of Science and Technology*, chapter Hysteresis. Academic Press, San Diego, California, USA, 1992.
- [18] Muijderman, Veldpaus, Van Heck, and Kok. A general criterion controller with preview for a semi-active truck suspension. In *Proceedings of the International Symposium on Advanced Vehicle Control AVEC 1996*, volume 1, pages 63–75, Aachen, Germany, June 1996.
- [19] J. H. E. A. Muijderman. *Flexible objective controllers for semi-active suspensions with preview*. PhD thesis, Eindhoven University of Technology, Eindhoven, The Netherlands, 1997.
- [20] J. Reimpel and H. Stoll. *Fahrwerktechnik: Stoß- und Schwingungsdämpfer*. VOGEL Buchverlag, Würzburg Germany, second and fully revised edition edition, 1989.
- [21] K. Reybrouck. A non linear parametric model of an automotive shock absorber. Technical Report 940869, SAE, 1994.
- [22] J-J.E. Slotine and W.Li. *Applied Nonlinear Control*. Prentice-Hall Inc., Englewood Cliffs, New Jersey, 1991.
- [23] G. Stephanopoulos. *Chemical Process Control*. PTR Prentice Hall, Englewood Cliffs, New Jersey, 1984.
- [24] C. Surace, K. Worden, and G.R. Tomlinson. On the non-linear characteristics of automotive shock absorbers. *Proceedings of the Institution of Mechanical Engineers, Part D*, pages 3–16, 1992.
- [25] G.A. Verbeek. *Nonlinear parametric identification using periodic equilibrium states: with application to an aircraft landing gear damper*. PhD thesis, Eindhoven University of Technology, Eindhoven, The Netherlands, 1993.
- [26] J. Wallaschek. Dynamics of non-linear automobile shock-absorbers. *International Journal Non-Linear Mechanics*, 25:299–308, 1990.
- [27] K. Worden. Data processing and experiment design for the restoring force surface method, part I: Integration and differentiation of measured time data. *Mechanical Systems and Signal Processing*, 4:295–319, 1990.
- [28] K. Worden. Data processing and experiment design for the restoring force surface method, part II: Choice of excitation signal. *Mechanical Systems and Signal Processing*, 4:321–344, 1990.
- [29] F. Wößner and P. Causemann. Continuously adjustable shock absorbers comparison, calculation and optimization. In *Proceedings of the International Symposium on Advanced Vehicle Control 1992*, pages 309–314, Yokohama/Tokyo, Japan, 1992.
- [30] M. Yamashita, K. Fujimori, K. Hayakawa, and H. Kimura. Application of H_∞ control to active suspension systems. In *IFAC'93*, volume 3, pages 143–146, 1993.
- [31] M. Yamashita, K. Fujimori, K. Hayakawa, and H. Kimura. Application of H_∞ control to active suspension systems. *Automatica*, 30(11):1717–1729, 1994.

A Used Symbols

Symbol	Unit	Description
α		Volumetric thermal-expansion coefficient
A_p	$[m^2]$	Cross sectional area of the piston
A_r	$[m^2]$	Cross sectional area of piston rod
A_{res}	$[m^2]$	Area of restriction
b	$[Ns/m]$	Linear damping constant
β'		Compressibility factor
C_d		Geometry effects of orifices
c_v	$[J/(kg K)]$	Specific heat at constant volume
Δp	$[Pa]$	Pressure difference
E	$[Nm]$	Energy / Dissipated energy
E	$[N]$	Tracking error in damper force
ϵ	$[-]$	Tracking error in damper setting
f	$[-]$	Internal damper setting
F	$[N]$	Realised damper force
F_d	$[N]$	Desired damper force
F_h	$[N]$	Damper force in "hard" setting
F_m	$[N]$	Measured damper force
F_s	$[N]$	Damper force in "soft" setting
hub	$[m]$	Excenter length in VDA-test
i	$[-]$	Integer number
Inf	$[-]$	Infinity (in Matlab)
k	$[N/m]$	Linear spring constant
K_d	$[-]$	Differential constant
K_i	$[-]$	Integral (reset) constant
K_p	$[-]$	Proportional constant
l_{tot}	$[m]$	Tube length
λ	$[W/K]$	thermal diffusivity
m	$[kg]$	Mass
n	$[-]$	Integer number
p	$[Pa]$	Pressure
p_{br}	$[Pa]$	Blow-off pressure at rebound
p_{rr}	$[Pa]$	Restriction pressure at rebound
ϕ_m	$[kg/s]$	Oil flow
ϕ_v	$[m^3/s]$	Oil flow

(Continued on next page)

symbol	Unit	description
q	$[m]$	Relative displacement
Q_g	$[J]$	Heat flow
q_{\max}	$[m]$	Maximum rod displacement, no space left for gas
R	$[J/(kg K)]$	Specific gas constant
ρ	$[kg/m^3]$	Density
rpm	$[(2\pi)/s]$	Revolutions per Minute (VDA-test)
s	$[m]$	Floating piston displacement
t	$[s]$	Time
T	$[K]$	Temperature
τ	$[s]$	Natural period of oscillation
τ_c	$[1/s]$	First order constant delay
t_d	$[s]$	Time lag (dead time)
$u(t)$		Input signal
v	$[V]$	Damper control voltage
v	$[m/s]$	Forward vehicle velocity
V	$[m^3]$	Volume
v_{sc}	$[V]$	Scaled damper control voltage
$W(f)$	$[-]$	Frequency domain weighing function
$x(t)$		General time-dependent signal
$y(t)$		General time-dependent signal
ζ	$[-]$	Damping factor
z	$[m]$	Chassis or axle displacement

Derivatives to time are denoted with an dot over the symbol, double derivatives have a double dot and triple derivatives use a triple dot. All other indexes are explained in the text

B White Box Model: used parameters

Geometry of the damper

It was chosen to use geometry data of the Biltstein B46 main tube as described in Reimpell und Stoll [20, Bild 5.1 and 2.24].

Note: all parameters are described for the damper at its maximum length: $q = 0[m]$.

description	symbol	value	unit
Piston rod area	A_r	$\frac{\pi}{4}0.017^2$	$[m^2]$
Piston area	A_p	$\frac{\pi}{4}0.046^2$	$[m^2]$
Tube length	l_{tot}	0.51	$[m]$
Gas length	$l_{tot} - s_0$	0.06	$[m]$
Volume Piston 1 (fixed)	V_{p1}	$0.01 A_r$	$[m^3]$
Volume Piston 2 (float)	V_{p2}	0	$[m^3]$

Data on fluidic contents of damper

The damper is filled with damper oil and nitrogen gas. These are material dependent parameters, followed by some constants which are derived from these and the geometry parameters. All parameters are defined for $T_0 = 293[K]$.

The oil density is defined for MONROE 18.00.01.06 damper oil.

Mass of the nitrogen gas was calculated solving a formula in order to obtain 50 [N]static damper force for $q = 0[m]$ and 450 [N]for $q = 0.4[m]$.

description	symbol	value	unit
Gas constant Nitrogen	R	296.8	$[J/kg K]$
thermal diffusivity	λ_g (Eq.(25))	7.9964	$[W/K]$
Oil density	ρ_{oil}	870	$[kg/m^3]$
Mass of Oil	m_{oil}	$\{s_0 A_p - V_{p1}\} \rho(T_0)$	$[kg]$
Mass of Nitrogen	m_g	$2.5873 \cdot 10^{-4}$	$[kg]$

The specific heat at constant volume c_v of the nitrogen gas was taken from Table D.5 from Janna [12].

Data on damper behaviour

The *blow-off* starts when the pressure difference Δp exceeds the blow-off pressure p_b . *Restriction* starts when the restriction pressure p_r is exceeded. Both pressures exists for *rebound* (p_{br} and p_{rr}) and *compression* (p_{bc} and p_{rc}). In the simulations, it was assumed that $p_{br} = p_{bc}$ and $p_{rr} = p_{rc}$.

These pressures were calculated from the demands:

- at $\dot{q} = 0.1[m/s]$, the blow-off starts for $F \approx 2500[N]$,
- at $\dot{q} = 1.1[m/s]$, the blow-off ends for $F \approx 8000[N]$.

resulting in:

description	symbol	value	unit
blow-off pressure	p_b	1.0910^6	$[Pa]$
restriction pressure	p_r	3.6410^6	$[Pa]$

C Damper warming in the VDA-test

Assume a sinusoidal excitation is applied to a shock absorber as discussed in Section 2.3.1. This excitation will result in damper warming.

To calculate this damper warming, some assumptions are made:

- the damper is assumed linear:

$$F = k \dot{q} = 10^4 \dot{q} \quad (56)$$

- all dissipated energy is converted into heat.
- all heat is used to warm the oil.
- no heat is exchanged with the surrounding air.

The dissipated energy in one period T with hub length hub and number of revolutions per minute rpm is:

$$E = \int_0^T F(\dot{q}(t)) \dot{q}(t) dt = 10^4 \int_0^{\frac{60}{rpm}} \dot{q}^2(t) dt = 333 \pi^2 rpm hub^2 \quad (57)$$

This heat is used to warm the oil. From Appendix B, the oil mass can be calculated: $0.68 [kg]$. This mass is used to calculate oil warming using:

$$\Delta T_{oil} = \frac{E}{m_{oil} c_{oil}} \quad (58)$$

For a hub length of $0.1 [m]$, the following damper oil heating were calculated:

$rpm [rev/min]$	$\dot{q}_{max} [m/s]$	$\Delta T_{oil} [K]$
25	0.26	0.64
50	0.52	1.27
75	0.78	1.91
100	1.04	2.54
150	1.57	3.8
200	2.1	5.1

Please note that damper cooling due to the exchange of heat with the surrounding air is not taken into account.

D Results of fitting second order systems

The first column contains the relative velocity, “C” (Compression) or “R” (Rebound). The notation $H \rightarrow S$ means stepping from the “hard” setting (3.235 [V]) to the “soft” setting (0.5 [V]).

			H \rightarrow S	S \rightarrow H	H \rightarrow M	M \rightarrow H	M \rightarrow S	S \rightarrow M
0.052	C	τ	0.0028	0.010	0.0037	0.006	0.0037	0.006
		ζ	0.6	0.65	0.33	0.65	0.60	0.65
		t_d	0.001	0.003	0	0	0	0.005
	R	τ	0.0032	0.016	0.0055	0.010	0.004	0.014
		ζ	0.55	0.8	⊖ 0.40	⊖ 0.75	⊖ 0.58	⊖ 0.82
		t_d	0.001	0.002	0	0	0	0.001
0.13	C	τ	0.003	0.005		0.0027	0.003	0.003
		ζ	0.65	0.7	⊙	0.6	0.6	0.65
		t_d	0	0.005		0.002	0	0.005
	R	τ	0.004	0.0035		0.004	0.035	0.006
		ζ	0.63	0.65	⊙	0.6	0.6	0.7
		t_d	0	0		0.002	0	0.005
0.26	C	τ	0.003	0.0032	0.003	0.0025	0.0032	0.003
		ζ	0.7	0.55	0.6	0.6	0.6	0.65
		t_d	0	0.006	0	0.001	0	0.005
	R	τ	0.004	0.005	0.003	0.0027	0.0035	0.0038
		ζ	0.6	0.6	0.45	0.42	0.55	0.58
		t_d	0	0.007	0	0.002	0.001	0.006
0.52	C	τ	0.003	0.003	0.0025	0.0028	0.003	0.003
		ζ	0.65	0.68	0.55	0.6	0.65	0.65
		t_d	0.001	0.005	0.001	0.002	0.001	0.005
	R	τ	0.0035	0.0035	0.003	0.0035	0.004	0.004
		ζ	0.7	0.6	0.45	0.45	0.65	⊖ 0.55
		t_d	0.001	0.001	0	0.002	0	0.005
1.0	C	τ	0.003	0.0038	0.002		0.003	0.0038
		ζ	0.8	0.7	0.65	⊙	0.7	0.65
		t_d	0	0.0095	0		0	0.008
	R	τ	0.0045	0.005	0.0045		0.0042	0.0045
		ζ	⊗ 0.8	0.6	0.85	⊙	0.8	0.7
		t_d	0	0.021	0.001		0.001	0.018

Comments:

- ⊖ Offset appears between f_d and f_{sim} . This was resolved by adjusting v .
- ⊗ This is not a second order behaviour. It seems first order.
- ⊙ The disturbances are too large to fit a curve. The result is only a rough estimation.

E Quarter Car model

A Quarter Car model was used to simulate the behaviour of a DAF 95 Truck. This model is derived from the model used by Huisman [9]. This model consists of two masses which are interconnected with an air spring and the ÖHLINS damper. This is depicted in Figure 40. The characteristic of the air spring can be found in Figure 41.

The tire model is a simplified version of the *Fixed Footprint Tire Model* as derived by Captain *et al.* [13] with parameters devised by Foag [6, Section 3.3.1]. It consists of a low-pass filter and a spring. The constant in the low-pass filter is defined:

$$\tau = \frac{\text{footprint}}{3v} \quad (59)$$

with the footprint as defined in Figure 40 in the detail and v as the the (forward) velocity.

The Quarter Car model outputs the relative acceleration $\ddot{z}_1 - \ddot{z}_2$ to the model of the ÖHLINS damper controller. The damper controller controls the model of the ÖHLINS damper and the resulting force is send back to the Quarter Car model. Note that the ÖHLINS damper output is doubled as *two* dampers will be mounted at each wheel to provide enough damping.

Model parameters:

chassis mass:	3721	[kg]
axle mass:	707	[kg]
tire stiffness:	2000	[kN/m]
footprint:	0.3	[m]

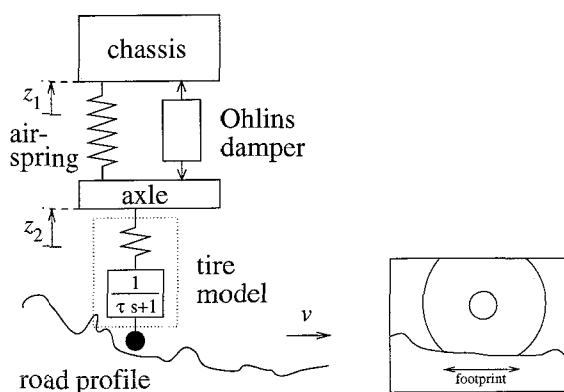


Figure 40: *Quarter Car model and footprint definition.*

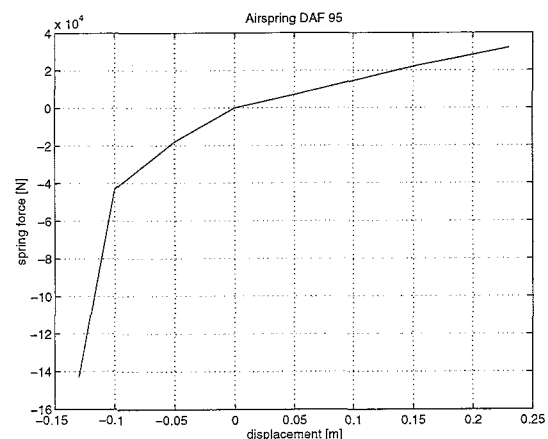


Figure 41: *Airspring characteristics.*